

Handling Concept Drift via Model Reuse

Peng Zhao, Le-Wen Cai, and Zhi-Hua Zhou*

National Key Laboratory for Novel Software Technology,

Nanjing University, Nanjing 210023, China

{zhaop, cailw, zhouzh}@lamda.nju.edu.cn

Abstract

In many real-world applications, data are often collected in the form of stream, and thus the distribution usually changes in nature, which is referred as *concept drift* in literature. We propose a novel and effective approach to handle concept drift via model reuse, leveraging previous knowledge by reusing models. Each model is associated with a weight representing its reusability towards current data, and the weight is adaptively adjusted according to the model performance. We provide generalization and regret analysis. Experimental results also validate the superiority of our approach on both synthetic and real-world datasets.

1 Introduction

With a rapid development in data collection technology, it is of great importance to analyze and extract knowledge from them. However, data are commonly in a streaming form and are usually collected from non-stationary environments, and thus they are evolving in nature. In other words, the joint distribution between the input feature and the target label will change, which is also referred as *concept drift* in literature [Gama *et al.*, 2014]. If we simply ignore the distribution change when learning from the evolving data stream, the performance will dramatically drop down, which are not empirically and theoretically suitable for these tasks. The concept drift problem has become one of the most challenging issues for data stream learning. It has gradually drawn researchers' attention to design effective and theoretically sound algorithms.

Data stream with concept drift is essentially almost impossible to learn (predict) if there is not any assumption on distribution change. That is, if the underlying distribution changes arbitrarily or even adversarially, there is no hope to learn a good model to make the prediction. We share the same assumption with most of the previous work, that is, *there contains some useful knowledge for future prediction in previous data*. No matter sliding window based approaches [Klinkenberg and Joachims, 2000; Bifet and Gavaldà, 2007; Kuncheva and Zliobaite, 2009], forgetting based approaches [Koychev, 2000; Klinkenberg, 2004] or ensemble based approaches [Kolter and Maloof, 2005, 2007; Sun *et al.*, 2018], they share the same assumption, whereas the only difference is how to utilize previous knowledge or data.

Another issue is that most previous work on handling concept drift focus on the algorithm design, only a few work consider the theoretical part [Helmbold and Long, 1994; Cramer *et al.*, 2010; Mohri and Medina, 2012]. There are some work proposing algorithms along with theoretical analysis, for example, Kolter and Maloof [2005] provides mistake and loss bounds and guarantees that the performance of the proposed approach is relative to the performance of the base learner. Harel *et al.* [2014] detects concept drift via resampling and provides the bounds on differentiates

*Corresponding author. Email: zhouzh@nju.edu.cn

based on stability analysis. However, seldom have clear theoretical guarantees, or justifications on why and how to leverage previous knowledge to fight with concept drift, especially from the generalization aspect.

In this paper, we propose a novel and effective approach for handling Concept Drift via model reuse, or CONDOR. It consists of two modules, ModelUpdate module aims at leveraging previous knowledge to help build the new model and update model pool, while WeightUpdate module adaptively assigns the weights for previous models according to their performance, representing the reusability towards current data. We justify the advantage of ModelUpdate from the aspect of generalization analysis, showing that our approach can benefit from a good weighted combination of previous models. Meanwhile, the WeightUpdate module guarantees that the weights will concentrate on the better-fit models. Besides, we also provide the dynamic regret analysis. Empirical experiments on both synthetic and real-world datasets validate the effectiveness of our approach.

In the following, Section 2 discusses related work. Section 3 proposes our approach. Section 4 presents theoretical analysis. Section 5 reports the experimental results. Finally, we conclude the paper and discuss future work in Section 6.

2 Related Work

CONCEPT DRIFT has been well-recognized in recent researches [Gama *et al.*, 2014; Gomes *et al.*, 2017]. Basically, if there is not any structural information about data stream, and the distribution can change arbitrarily or even adversarially, we shall not expect to learn from historical data and make any meaningful prediction. Thus, it is crucial to make assumptions about the concept drift stream. Typically, most previous work assume that the nearby data items contain more useful information w.r.t. the current data, and thus researchers propose plenty of approaches based on the *sliding window* and *forgetting* mechanisms. Sliding window based approaches maintain the nearest data items and discard old items, with a fixed or adaptive window size [Klinkenberg and Joachims, 2000; Kuncheva and Zliobaite, 2009]. Forgetting based approaches do not explicitly discard old items but downweight previous data items according to their age [Koychev, 2000; Klinkenberg, 2004]. Another important category falls into the *ensemble* based approaches, as they can adaptively add or delete base classifiers and dynamically adjust weights when dealing with evolving data stream. A series work borrows the idea from boosting [Schapire, 1990] and online boosting Beygelzimer *et al.* [2015], dynamically adjust weights of classifiers. Take a few representatives, dynamic weighted majority (DWM) dynamically creates and removes weighted experts in response to changes [Kolter and Maloof, 2003, 2007]. Additive expert ensemble (AddExp) maintains and dynamically adjusts the additive expert pool, and provides the theoretical guarantee with solid mistake and loss bounds [Kolter and Maloof, 2005]. Learning in the non-stationary environments (Learn⁺⁺.NSE) trains one new classifier for each batch of data it receives, and combines these classifiers [Elwell and Polikar, 2011]. There are plenty of approaches to learning or mining from the evolving data stream, readers can refer to a comprehensive survey [Gama *et al.*, 2014; Gomes *et al.*, 2017]. As for boosting and ensemble approaches, readers are recommended to read the books [Schapire and Freund, 2012; Zhou, 2012].

Our approach is kind of similar to DWM and AddExp on the surface. We all maintain a model pool and adjust weights to penalty models with poor performance. However, we differ from the model update procedure and they ignore to leverage previous knowledge and reuse models to help build new model and update model pool. Besides, our weight update strategies are also different.

MODEL REUSE is an important learning problem, also named as model transfer, hypothesis transfer learning, or learning from auxiliary classifiers. The basic setting is that one desires to reuse pre-trained models to help further model building, especially when the data are too scarce to directly train a fair model. A series work lies in the idea of *biased regularization*, which leverages previous models as the bias regularizer into empirical risk minimization, and achieves a good performance in plenty of scenarios [Duan *et al.*, 2009; Tommasi *et al.*, 2010, 2014]. There are also some other attempts and applications like model reuse by random forests [Segev *et al.*, 2017], and applying model reuse to adapt different performance measures [Li *et al.*, 2013]. Apart from algorithm design, theoretical foundations are recently established by stability [Kuzborskij and Orabona, 2013], Rademacher complexity [Kuzborskij and Orabona, 2017] and transformation functions [Du *et al.*, 2017].

Our paper proposes to handle concept drift problem via utilizing model reuse learning. The idea of leveraging previous knowledge is reminiscent of some previous work coping with concept drift by model reuse (transfer), like the temporal inductive transfer (TIX) approach [Forman, 2006] and the diversity and transfer-based ensemble learning (DTEL) approach [Sun *et al.*, 2018]. Both of them are batch-style approaches, that is, they need to receive a batch of data each time, whereas ours can update either in an incremental style or a batch update mode. TIX concatenates the predictions from previous models into the feature of next data batch as the new data, and a new model is learned from the augmented data batch. DTEL chooses decision tree as the base learner, and builds a new tree by “fine-tuning” previous models by a direct tree structural adaptation. It maintains a fixed size model pool with the selection criteria based on diversity measurement. They both do not depict the reusability of previous models, which is carried out by `WeightUpdate` module in our approach. Last but not the least important, our approach is proposed with sound theoretical guarantees, in particular, we carry out a generalization justification on why and how to reuse previous models. Nevertheless, theirs are not theoretically clear in general.

3 Proposed Approach

In this section, we first illustrate the basic idea, and then identify two important modules in designing our proposed approach, i.e., `ModelUpdate` and `WeightUpdate`.

Specifically, we adopt a drift detection algorithm to split the whole data stream into epochs in which the distribution underlying is relatively smooth, and we only do the model update when detecting the concept drift or achieving the maximum update period p . As shown in Figure 1, the drift detector \mathcal{D} will monitor the concept drift. When the drift is detected, instead of resetting the model pool and incrementally training a new model, we aim at leveraging the knowledge in previous models to enhance the overall performance by alleviating the cold start problem.

Basically, our approach consists of two important modules,

- (1) `ModelUpdate` by model reuse: we leverage previous models to build the new model and update model pool, by making use of biased regularization multiple model reuse.
- (2) `WeightUpdate` by expert advice: we associate each previous model with a weight representing the reusability towards current data. The weights are updated according to the performance of each model, in an exponential weighted average manner.

3.1 Model Update by Model Reuse

We leverage previous models to adapt the current data epoch via model reuse by *biased regularization* [Schölkopf *et al.*, 2001; Tommasi *et al.*, 2014].

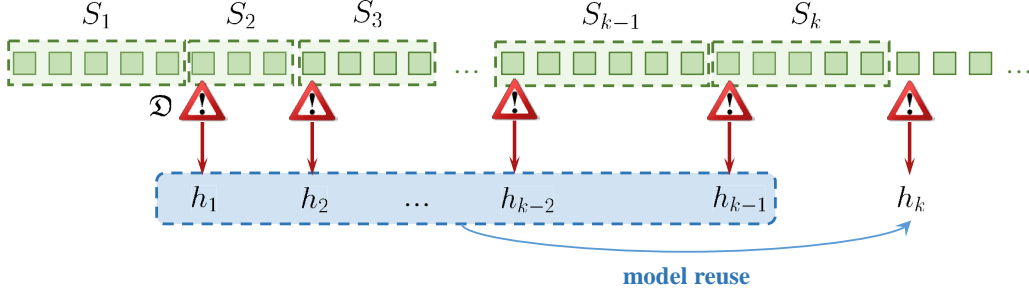


Figure 1: Illustration of main idea: on one hand, we utilize the data items in current epoch S_k ; on the other hand, we leverage the previous knowledge ($\{h_1, h_2, \dots, h_{k-1}\}$) via model reuse.

Consider the k -th model update as illustrated in Figure 1, we desire to leverage previous models $\{h_1, \dots, h_{k-1}\}$ and current data epoch S_k to obtain a new model h_k . With a slight abuse of notation, we denote $S_k = \{(x_1, y_1), \dots, (x_m, y_m)\}$. In this paper, we adopt linear classifier as the base model, and the model reuse by biased regularization can be formulated as

$$\hat{\mathbf{w}}_k = \arg \min_{\mathbf{w}} \left\{ \frac{1}{m} \sum_{i=1}^m \ell(\langle \mathbf{w}, \mathbf{x}_i \rangle, y_i) + \mu \Omega(\mathbf{w} - \mathbf{w}_p) \right\}, \quad (1)$$

where $\ell : \mathcal{Y} \times \mathcal{Y} \rightarrow \mathbb{R}_+$ is the loss function, and $\Omega : \mathcal{H} \rightarrow \mathbb{R}_+$ is the regularizer. Besides, $\mu > 0$ is a positive trade-off regularization coefficient, and \mathbf{w}_p is the linear weighted combination of previous models, namely, $\mathbf{w}_p = \sum_{j=1}^{k-1} \beta_j \hat{\mathbf{w}}_j$, where β_j is the weight associated with previous model h_j , representing the reusability of each model on current data epoch.

For simplicity, in this paper, we choose the square loss with ℓ_2 regularization in practical implementation, essentially, Least Square Support Vector Machine (LS-SVM) [Suykens *et al.*, 2002]. It is shown [Suykens *et al.*, 2002] that the optimal solution can be expressed as $\mathbf{w} = \sum_{i=1}^m \alpha_i \mathbf{x}_i$, with $\boldsymbol{\alpha} = [\alpha_1, \dots, \alpha_m]^T$ solved by

$$\begin{bmatrix} \mathbf{K} + \frac{1}{\mu} \mathbf{I} & \mathbf{1} \\ \mathbf{1} & 0 \end{bmatrix} \begin{bmatrix} \boldsymbol{\alpha} \\ b \end{bmatrix} = \begin{bmatrix} \mathbf{y} - \sum_{j=1}^{k-1} \beta_j \hat{\mathbf{y}}_j \\ 0 \end{bmatrix}, \quad (2)$$

where \mathbf{K} is the linear kernel matrix, i.e., $\mathbf{K}_{ij} = \mathbf{x}_i^T \mathbf{x}_j$. Besides, \mathbf{y} and $\hat{\mathbf{y}}_j$ are the vectors containing labels of data stream and predictions of the previous j -th model, that is, $\mathbf{y} = [y_1, \dots, y_m]^T$ and $\hat{\mathbf{y}}_j = [\langle \hat{\mathbf{w}}_j, \mathbf{x}_1 \rangle, \dots, \langle \hat{\mathbf{w}}_j, \mathbf{x}_m \rangle]^T$.

If the concept drift occurs very frequently or data stream accumulates for a long time, the size of model pool will explode supposing there is no delete operation. Thus, we set the maximum of model pool size as K . Apparently, we can keep K of all models with largest diversity as done in [Sun *et al.*, 2018]. For simplicity, we only keep the newest K ones in the model pool.

Remark 1. The biased regularization model reuse learning (1) is not limited in binary scenario, and can be easily extended to multi-class scenario as,

$$\hat{W} = \arg \min_W \left\{ \frac{1}{m} \sum_{i=1}^m \ell(\rho_{h_{W,p}}(\mathbf{x}_i, y_i)) + \mu \Omega(W) \right\}, \quad (3)$$

where $h_{W,p}(\mathbf{x}) = W^T \mathbf{x} + h_p(\mathbf{x})$, and $\rho_h(\mathbf{x}, y)$ is the margin. We defer the notations and corresponding theoretical analyses in Section C. In addition, our approach is a framework, and can choose

Algorithm 1 CONDOR

Input: Data stream $\{(\mathbf{x}_1, y_1), \dots, (\mathbf{x}_T, y_T)\}$. Drift detector $\mathcal{D}(\delta, \mathbf{x}, y)$ with corresponding threshold δ ; step size η ; maximum update period (epoch size) p ; model pool size K .

Output: Prediction \hat{y}_t , where $t = 1, \dots, T$; and returned model pool \mathcal{H} .

- 1: Initialize model on first (or a couple of) data items: $h_1 \leftarrow \text{Train}(\mathbf{x}_1)$, and $\mathcal{H} \leftarrow \{h_1\}$;
- 2: Initialize weight $\beta_{1,1} \leftarrow 1$;
- 3: **for** $t = 1$ **to** T **do**
- 4: Receive \mathbf{x}_t ;
- 5: **for** $k = 1$ **to** $|\mathcal{H}|$ **do**
- 6: $\hat{y}_{t,k} \leftarrow h_k(\mathbf{x}_t)$;
- 7: **end for**
- 8: $\hat{y}_t \leftarrow \sum_{k=1}^{|\mathcal{H}|} \beta_{t,k} \hat{y}_{t,k} / \sum_{k=1}^{|\mathcal{H}|} \beta_{t,k}$;
- 9: Receive y_t ;
- 10: **for** $k = 1$ **to** $|\mathcal{H}|$ **do**
- 11: $\beta_{t+1,k} \leftarrow \beta_{t,k} \exp\{-\eta \ell(\hat{y}_{t,k}, y_t)\}$; // WeightUpdate
- 12: **end for**
- 13: **if** $\mathcal{D}(\delta, \mathbf{x}_t, y_t) > 0$ or $(t \bmod p = 0)$ **then**
- 14: $h \leftarrow \text{ModelUpdate}(S_{|\mathcal{H}|}, \mathcal{H}, \{\beta_1, \dots, \beta_{|\mathcal{H}|}\})$;
- 15: $\mathcal{H} \leftarrow \mathcal{H} \cup \{h\}$;
- 16: **if** $|\mathcal{H}| > K$ **then**
- 17: Remove the oldest model from \mathcal{H} .
- 18: **end if**
- 19: **for** $k = 1$ **to** $|\mathcal{H}|$ **do**
- 20: Initialize the weights: $\beta_{1,k} \leftarrow 1/|\mathcal{H}|$;
- 21: **end for**
- 22: **end if**
- 23: **end for**

any multiple model reuse algorithm as the sub-routine. For instance, we can also choose model reuse by random forests [Segev *et al.*, 2017].

3.2 Weight Update by Expert Advice

After ModelUpdate step, the weight distribution in the model pool \mathcal{H} will reinitialize. We adopt a uniform initialization: $\beta_{1,k} = 1/|\mathcal{H}|$, for $k = 1, \dots, |\mathcal{H}|$.

After the initialization, we update weight of each model by expert advice [Cesa-Bianchi and Lugosi, 2006]. Specifically, when the new data item comes, we receive \mathbf{x}_t and each previous model will provide its prediction $\hat{y}_{t,k}$, and the final prediction \hat{y}_t is made based on the weighted combination of expert advice ($\hat{y}_{t,k}$ s). Next, the true label is revealed as y_t , and we will update the weights according to the loss each model suffers, in an exponential weighted manner,

$$\beta_{t+1,k} \leftarrow \beta_{t,k} \exp\{-\eta \ell(\hat{y}_{t,k}, y_t)\}.$$

The overall procedure of proposed approach CONDOR is summarized in Algorithm 1.

4 Theoretical Analysis

In this section, we provide theoretical analysis both locally and globally.

- (1) Local analysis: consider both generalization and regret aspects on each epoch locally;
- (2) Global analysis: examine regret on the whole data stream globally.

Besides, in local analysis, we also provide the multi-class model reuse analysis, and we let it an independent subsection to better present the results.

4.1 Local Analysis

The local analysis means that we scrutinize the performance on a particular epoch. On one hand, we are concerned about the generalization ability of the model obtained by `ModelUpdate` module. Second, we study the quality of learned weights by `WeightUpdate` module and the cumulative regret of prediction.

Let us consider the epoch S_k , the `ModelUpdate` module reuses previous models h_1, \dots, h_{k-1} to help built new model h_k , as shown in Figure 1. To simplify the presentation, we introduce some notations. Suppose the length of data stream S is T , and is partitioned into k epochs, S_2, \dots, S_k .¹ For epoch S_k , we assume the distribution is identical, i.e., S_k is a sample of m_k points drawn i.i.d. according to distribution \mathcal{D}_k , where m_k denotes its length.

First, we conduct generalization analysis on `ModelUpdate` module. Define the risk and empirical risk of hypothesis (model) h on epoch S_k by

$$R(h) = \mathbb{E}_{(\mathbf{x}, y) \sim \mathcal{D}_k} [\ell(h(\mathbf{x}), y)], \quad \hat{R}(h) = \frac{1}{m_k} \sum_{i \in S_k} \ell(h(\mathbf{x}_i), y_i).$$

Here, with a slight abuse of notations, we also adopt S_k to denote the index included in the epoch, and $\hat{R}(h)$ instead of $\hat{R}_{S_k}(h)$ for simplicity. The new model h_k is built and updated on epoch S_k via `ModelUpdate` module, then we have the following generalization error bound.

Theorem 1. Assume that the non-negative loss function $\ell : \mathcal{Y} \times \mathcal{Y} \rightarrow \mathbb{R}_+$ is bounded by $M \geq 0$, and is L -Lipschitz continuous. Also, assume the regularizer $\Omega : \mathcal{H} \rightarrow \mathbb{R}_+$ is a non-negative and λ -strongly convex function w.r.t. a norm $\|\cdot\|$. Given the model pool $\{h_1, h_2, \dots, h_{k-1}\}$ with $\mathbf{h}_p(\mathbf{x}) := [h_1(\mathbf{x}), h_2(\mathbf{x}), \dots, h_{k-1}(\mathbf{x})]^\top$, and denote h_p be a linear combination of previous models, i.e., $h_p(\mathbf{x}) = \langle \boldsymbol{\beta}, \mathbf{h}_p(\mathbf{x}) \rangle$ and supposing $\Omega(\boldsymbol{\beta}) \leq \rho$ and $\rho = O(1/m)$. Let h_k be the model returned by `ModelUpdate`. Then, for any $\delta > 0$, with probability at least $1 - \delta$, the following holds,²

$$R(h_k) - \hat{R}(h_k) \leq 4L\sqrt{\frac{\epsilon_1}{m}} + 3\sqrt{\frac{\epsilon_2 \log(1/\delta)}{m}} + \frac{3M \log(1/\delta)}{4m},$$

where $\epsilon_1 = \frac{B^2 R_p}{\lambda \mu} + \frac{C^2 \rho}{\lambda}$ and $\epsilon_2 = \frac{M}{4} R_p + 4LM\sqrt{\frac{B^2 R_p + C^2 \mu \rho}{\lambda \mu m}}$. Besides, $B = \sup_{\mathbf{x} \in \mathcal{X}} \|\mathbf{x}\|_*$ and $C = \sup_{\mathbf{x} \in \mathcal{X}} \|\mathbf{h}_p(\mathbf{x})\|_*$.

To better present the results, we only keep the leading term w.r.t. m and R_p , and we have

$$R(h_k) - \hat{R}(h_k) = O\left(\frac{1}{\sqrt{m}} \left(\sqrt{R_p} + \sqrt{\frac{R_p}{\lambda \mu}} + \sqrt[4]{\frac{R_p}{\lambda \mu m}}\right) + \frac{1}{m} \left(\sqrt{\frac{1}{\lambda}} + \sqrt[4]{\frac{1}{\lambda}}\right)\right), \quad (4)$$

where $R_p = R(h_p) = \mathbb{E}_{S_k}[\ell(h_p)]$, representing the risk of reusing model on current distribution.

To better present our main result, we defer the proof of Theorem 1 in Appendix B.

¹Here, we start from epoch 2, since the first epoch cannot utilize `WeightUpdate`.

²We use m instead of m_k for simplicity.

Remark 2. Eq. (4) shows that ModelUpdate procedure enjoys an $O(1/\sqrt{m})$ generalization bound under certain conditions. In particular, when the previous models are sufficiently good, that is, have a small risk on the current distribution \mathcal{D}_k (i.e., when $R_p \rightarrow 0$), we can obtain an $O(1/m)$ bound, a fast rate convergence guarantee. This implies the effectiveness of leveraging and reusing previous models to current data, especially if we can reuse previous models properly (as we will illustrate in the following paragraph).

Remark 3. The main techniques in the proof are inspired by Kuzborskij and Orabona [2017], but we differ in two aspects. First, we only assume the Lipschitz condition, and thus their results are not suitable under our conditions. Second, we extended the analysis of model reuse to multi-class scenarios, and include the results in Appendix C for a better presentation.

Before the next presentation, we need to introduce more notations. Let L_T be as the global cumulative loss on the whole data stream S . on epoch S_k , let L_{S_k} be as the local cumulative loss suffered by our approach, and $L_{S_k}^{(j)}$ as the local cumulative loss suffered by the previous model h_j ,

$$L_T = \sum_{i=1}^T \ell(\hat{y}_i, y_i), \quad L_{S_k} = \sum_{i \in S_k} \ell(\hat{y}_i, y_i), \quad L_{S_k}^{(j)} = \sum_{i \in S_k} \ell(h_j(\mathbf{x}_i), y_i). \quad (5)$$

Next, we show WeightUpdate returns a good weight distribution, implying our approach can reuse previous models properly. In fact, we have the following observation regarding to weight distribution.

Observation 1 (Weight Concentration). *During the WeightUpdate procedure in epoch S_k , the weights will concentrate on those previous models who suffer a small cumulative loss on S_k .*

Proof. By a simple analysis on the WeightUpdate procedure, we know that the weight associated with the j -th previous model is equal to $\beta_{1,j} \exp\{-\eta L_{S_k}^{(j)}\}$, where $j = 1, \dots, k-1$. \square

Though the observation seems quite straightforward, it plays an important role in making our approach successful. The statement guarantees that the algorithm adaptively assigns more weights on better-fit previous models, which essentially depicts the ‘reusability’ of each model. We also conduct additional experiments to support this point in Appendix D.1.

Third, we show that our approach can benefit from *recurring concept drift* scenarios. Here, we adopt the concept of *cumulative regret* (or *regret*) from online learning [Zinkevich, 2003] as the performance measurement.

Theorem 2 (Improved Local Regret [Cesa-Bianchi and Lugosi, 2006]). Assume that the loss function $\ell : \mathcal{Y} \times \mathcal{Y} \rightarrow \mathbb{R}_+$ is convex in its first argument and takes the values in $[0, 1]$. Besides, the step size is set as $\eta = \ln(1 + \sqrt{2 \ln(k-1)/L_{j_k}^*})$, where $L_{j_k}^* = \min_{j=1, \dots, k-1} L_{S_k}^{(j)}$ is the cumulative loss of the best-fit previous model and is supposed to be known in advance. Then, we have,

$$\text{Regret}_{S_k} = L_{S_k} - L_{j_k}^* \leq \sqrt{2L_{j_k}^* \ln(k-1)} + \ln(k-1).$$

Proof. Refer to the proof presented in page 21 in Chapter 2.4 of Cesa-Bianchi and Lugosi [2006]. \square

Above statement shows that the order of regret bound can be substantially improved from a typical $O(m_k)$ to $O(\ln k)$, independent from the number of data items in the epoch, providing $L_{j_k}^* \ll \sqrt{m_k}$, that is, the cumulative loss of the best-fit previous model is small.

Remark 4. Theorem 2 implies that if the concept of epoch S_k or a similar concept has emerged previously, our approach enjoys a substantially improved local regret providing a proper step size is chosen. This accords to our intuition on why model reuse helps for concept drift data stream. In many situations, although the distribution underlying might change over time, the concepts can be recurring, i.e., disappear and re-appear [Katakis *et al.*, 2010; Gama and Kosina, 2014]. Thus, the statement shows that our approach can benefit from such recurring concepts, and we empirically support this point in Appendix D.2.

4.2 Global Analysis

The global analysis means that we study the overall performance on the whole data stream. We provide the global dynamic regret as follows.

Theorem 3 (Global Dynamic Regret). Assume that the loss function $\ell : \mathcal{Y} \times \mathcal{Y} \rightarrow \mathbb{R}_+$ is convex in its first argument and takes the values in $[0, 1]$. Assume that the step size in S_k epoch is set as $\eta_k = \sqrt{(8 \ln(k-1))/m_k}$ ³, then we have

$$\text{Regret}_T = L_T - \sum_{k=2}^K L_{j_k^*} \leq \sqrt{\left(\sum_{k=1}^{K-1} \ln k\right) T/2}, \quad (6)$$

where $j_k^* = \arg \min_{j=1, \dots, k-1} L_{S_k}^{(j)}$.

The proof of global dynamic regret is built on the local static regret analysis in each epoch. And we can see that for data stream with a fix length T , the more concept drifts occur (i.e., larger K), the larger the regret will be. This accords with our intuition, on one hand, the sum of best-fit local cumulative loss ($\sum_{k=2}^K L_{j_k^*}$) is going to be compressed with more previous models. On the other hand, the learning problem becomes definitely harder as concept drift occurs more frequently.

Our `WeightUpdate` strategy is essentially exponentially weighted average forecaster [Cesa-Bianchi and Lugosi, 2006], and thus we have the following local regret guarantee in each epoch.

Lemma 1 (Theorem 2.2 in Cesa-Bianchi and Lugosi [2006]). Assume that the loss function $\ell : \mathcal{Y} \times \mathcal{Y} \rightarrow \mathbb{R}_+$ is convex in its first argument and takes the values in $[0, 1]$. Assume that the step size is set as $\eta = \sqrt{8 \ln(k-1)/m_k}$, then we have

$$L_{S_k} \leq \min_{j=1, \dots, k-1} L_{S_k}^{(j)} + \sqrt{(m_k/2) \ln(k-1)}.$$

Proof. The proof is based on a simple reduction from our scenario to standard *exponentially weighted average forecaster*. For epoch S_k , let previous models pool $\{h_1, h_2, \dots, h_{k-1}\}$ be as the expert pool. Then, plugging the expert number $N = k-1$ and number of instances $n = m_k$ into Theorem 2.2 in Cesa-Bianchi and Lugosi [2006], we obtain the statement.

Besides, the proof of exponentially weighted average forecaster is standard, which utilizes *potential function method* [Cesa-Bianchi and Lugosi, 2006; Mohri *et al.*, 2012]. For a detailed proof, one can refer to the proof presented in page 157-159 in Chapter 7 of book [Mohri *et al.*, 2012]. \square

Now, we proceed to prove Theorem 3.

³The choice of η requires the knowledge of epoch size, which can be eliminated by *doubling trick*, at the price of a small constant factor [Cesa-Bianchi *et al.*, 1997].

Proof. Our proof relies on the application of local static regret analysis. Since S_2, \dots, S_K is a partition of the whole period T , we apply Lemma 1 on each epoch locally and obtain

$$L_{S_k} \leq \min_{j=1, \dots, k-1} L_{S_k}^{(j)} + \sqrt{(m_k/2) \ln(k-1)}. \quad (7)$$

Sum over the index of j from 1 to $k-1$, we have

$$\begin{aligned} L_T &= \sum_{k=2}^K L_{S_k} \\ &\leq \sum_{k=2}^K L_{j_k^*} + \sum_{k=2}^K \sqrt{(m_k/2) \ln(k-1)} \end{aligned} \quad (8)$$

$$\begin{aligned} &\leq \sum_{k=2}^K L_{j_k^*} + \sqrt{\sum_{k=2}^K (m_k/2) \sum_{k=2}^K \ln(k-1)} \\ &= \sum_{k=2}^K L_{j_k^*} + \sqrt{\left(\sum_{k=1}^{K-1} \ln k \right) T/2} \end{aligned} \quad (9)$$

where (8) holds by substituting (7) into each epoch S_k , and (9) holds by applying Cauchy-Schwartz inequality. \square

Remark 5. Essentially, the regret bound in (6) is different from the traditional (static) regret bound. It measures the difference between the global cumulative loss with the sum of local cumulative loss suffered by previous best-fit models. Namely, our competitor changes in each epoch, which depicts the distribution change in the sequence, and thus is more suitable to be the performance measurement in non-stationary environments.

4.3 Multi-Class Model Reuse Learning

In multi-class learning scenarios, the notations are slightly different from those in binary case. We first introduce the new notations for a clear presentation.

Let \mathcal{X} denote the input feature space and $\mathcal{Y} = \{1, 2, \dots, c\}$ denote the target label space. Our analysis acts on the last data epoch $S_k = \{(\mathbf{x}_1, y_1), \dots, (\mathbf{x}_{m_k}, y_{m_k})\}$, a sample of m_k points drawn i.i.d. according to distribution \mathcal{D}_k , where $\mathbf{x}_i \in \mathbb{R}^d$ and $y_i \in \mathcal{Y}$ with only a single class from $\{1, \dots, c\}$. Given the multi-class hypothesis set \mathcal{H} , any hypothesis $h \in \mathcal{H}$ maps from $\mathcal{X} \times \mathcal{Y} \rightarrow \mathbb{R}$, and makes the prediction by $\mathbf{x} \rightarrow \arg \max_{y \in \mathcal{Y}} h(\mathbf{x}, y)$. This naturally rises the definition of *margin* $\rho_h(\mathbf{x}, y)$ of the hypothesis h at a labeled instance (\mathbf{x}, y) ,

$$\rho_h(\mathbf{x}, y) = h(\mathbf{x}, y) - \max_{y' \neq y} h(\mathbf{x}, y').$$

The non-negative loss function $\ell : \mathbb{R} \rightarrow \mathbb{R}$ is bounded by $M > 0$. Besides, we assume the loss function is *regular loss* defined in Lei *et al.* [2015].

Definition 1 (Regular Loss). We call a loss function $\ell : \mathbb{R} \rightarrow \mathbb{R}$ is a L -regular if it satisfies the following properties (Cf. Definition 2 in Lei *et al.* [2015]):

- (i) $\ell(t)$ bounds the 0-1 loss from above: $\ell(t) \geq \mathbf{1}_{t \leq 0}$;
- (ii) $\ell(t)$ is L -Lipschitz continuous, i.e., $|\ell(t_1) - \ell(t_2)| \leq L|t_1 - t_2|$;

(iii) $\ell(t)$ is decreasing and it has a zero point c_ℓ , i.e., there exists a c_ℓ such that $\ell(c_\ell) = 0$.

Then the risk and empirical risk of a hypothesis h on epoch S_k are defined by

$$R(h) = \mathbb{E}_{(\mathbf{x}, y) \sim \mathcal{D}_k} [\mathbf{1}_{\rho_h(\mathbf{x}, y) \leq 0}], \quad \hat{R}_S(h) = \frac{1}{m_k} \sum_{i \in S_k} \ell(\rho_h(\mathbf{x}_i, y_i)).$$

Our goal is to provide a generalization analysis, namely, to prove that risk $R(h)$ approaches empirical risk $\hat{R}(h)$ as number of instances m_k increases, and establish the convergence rate. Since $\mathbb{E}_{(\mathbf{x}, y) \sim \mathcal{D}_k} [\hat{R}(h)] \neq R(h)$, thus, we cannot directly utilize concentration inequalities to help analysis. To make this simpler, we need to introduce the risk w.r.t. loss function ℓ ,

$$R_\ell(h) = \mathbb{E}_{(\mathbf{x}, y) \sim \mathcal{D}_k} [\ell(\rho_h(\mathbf{x}, y))].$$

From property (iii) in Definition 1, we know that the risk $R(h)$ is a lower bound on $R_\ell(h)$, that is $R(h) \leq R_\ell(h)$. Thus, we only need to establish generalization bound between $R_\ell(h)$ and $\hat{R}(h)$. Apparently, $\mathbb{E}_{(\mathbf{x}, y) \sim \mathcal{D}_k} [\hat{R}(h)] = R_\ell(h)$, thus we can utilize concentration inequalities again.

First, we identify the optimization formulation of multi-class biased regularization model reuse,

$$\hat{W} = \arg \min_W \left\{ \frac{1}{m} \sum_{i=1}^m \ell(\rho_{h_{W,p}}(\mathbf{x}_i, y_i)) + \lambda \Omega(W) \right\}, \quad (10)$$

where $h_{W,p}(\mathbf{x}) = W^\top \mathbf{x} + h_p(\mathbf{x})$.

We specify the regularizer as square of Frobenius norm, namely, $\Omega(W) = \|W\|_F^2$, and provide the following generalization error bound.

Theorem 4. Let $H \subseteq \mathbb{R}^{\mathcal{X} \times \mathcal{Y}}$ be a hypothesis set with $\mathcal{Y} = \{1, 2, \dots, c\}$. Assume that the non-negative loss function $\ell : \mathbb{R} \rightarrow \mathbb{R}_+$ is L -regular. Given the model pool $\{h_1, h_2, \dots, h_{k-1}\}$ with $\mathbf{h}_p(\mathbf{x}) := [h_1(\mathbf{x}), h_2(\mathbf{x}), \dots, h_{k-1}(\mathbf{x})]^\top$, and denote h_p be a linear combination of previous models, i.e., $h_p(\mathbf{x}) = \langle \boldsymbol{\beta}, \mathbf{h}_p(\mathbf{x}) \rangle$ and supposing $\|\boldsymbol{\beta}\|^2 \leq 2\rho$ and $\rho = O(1/m)$. Let h_k be the model returned by ModelUpdate. Then, for any $\delta > 0$, with probability at least $1 - \delta$, the following holds,⁴

$$R(h_{\hat{W},p}) - \hat{R}_S(h_{\hat{W},p}) \leq 2Lc^2 \sqrt{\frac{\epsilon_1}{m}} + 3\sqrt{\frac{\epsilon_2 \log(1/\delta)}{4m}} + \frac{3M \log(1/\delta)}{4m}.$$

where $\epsilon_1 = \frac{2B^2 LR_p}{\lambda} + C^2 \rho$ and $\epsilon_2 = M \left(8Lc^2 \sqrt{\frac{2(B^2 R_p + C^2 \lambda \rho)}{\lambda m}} + R_p \right)$. Besides, $B = \sup_{\mathbf{x} \in \mathcal{X}} \|\mathbf{x}\|$ and $C = \sup_{\mathbf{x} \in \mathcal{X}} \|\mathbf{h}_p(\mathbf{x})\|$.

To better present the results, we only keep the leading term w.r.t. m and R_p , and we have

$$R(h_k) - \hat{R}(h_k) = O \left(\frac{c^2}{\sqrt{m}} \left(\sqrt{R_p} + \sqrt{\frac{LR_p}{\lambda}} + \sqrt[4]{\frac{L^2 R_p}{\lambda m}} \right) + \frac{1}{m} \sqrt[4]{\frac{1}{\lambda}} \right), \quad (11)$$

where $R_p = R(h_p) = \mathbb{E}_{S_k} [\ell(h_p)]$, representing the risk of reusing model on current distribution.

Remark 6. From Theorem 4, we can see that the main result and conclusion in multi-class case is very similar to that in binary case. In (11), we can see that CONDOR enjoys an $O(1/\sqrt{m})$ order generalization bound, which is consistent to the common learning guarantees. More importantly, CONDOR enjoys an $O(1/m)$ order fast rate generalization guarantees, when $R_p \rightarrow 0$, namely, when the previous model h_p is highly ‘reusable’ with respect to the current data. This shows the effectiveness of leveraging and reusing previous models to help build new model in CONDOR, in multi-class scenarios.

⁴We use m instead of m_k for simplicity.

5 Experiments

In this section, we examine the effectiveness of CONDOR on both synthetic and real-world concept drift datasets. Additional experimental regarding to weight concentration, recurring concept drift, parameter study and robustness comparisons are presented in Appendix D.

Compared Approaches. We conduct the comparisons with two classes of state-of-the-art concept drift approaches. The first class is the *ensemble category*, including (a) Learn⁺⁺.NSE [Elwell and Polikar, 2011], (b) DWM [Kolter and Maloof, 2003, 2007] and (c) AddExp [Kolter and Maloof, 2005]. The second class is the *model-reuse category*, including (d) DTEL [Sun *et al.*, 2018] and (e) TIX [Forman, 2006]. Essentially, DTEL and TIX also adopt ensemble idea, we classify them into model-reuse category just to highlight their model reuse strategies.

Settings. In our experiments, we choose ADWIN algorithm [Bifet and Gavaldà, 2007] as the the drift detector \mathcal{D} with default parameter setting reported in their paper and source code. Besides, for all the approaches, we set the maximum update period (epoch size) $p = 50$,⁵ and model pool size $K = 25$.

Table 1: Basic statistics of datasets with concept drift.

Dataset	# instance	# dim	# class	Dataset	# instance	# dim	# class
SEA200A	24,000	3	2	GEARS-2C-2D	200,000	2	2
SEA200G	24,000	3	2	Usenet-1	1,500	100	2
SEA500G	60,000	3	2	Usenet-2	1,500	100	2
CIR500G	60,000	3	2	Luxembourg	1,900	32	2
SINE500G	60,000	2	2	Spam	9,324	500	2
STA500G	60,000	3	2	Email	1,500	913	2
1CDT	16,000	2	2	Weather	18,159	8	2
1CHT	16,000	2	2	GasSensor	4,450	129	6
UG-2C-2D	100,000	2	2	Powersupply	29,928	2	2
UG-2C-3D	200,000	3	2	Electricity	45,312	8	2
UG-2C-5D	200,000	5	2	Covertypes	581,012	54	2

Synthetic Datasets. As it is not realistic to foreknow the detailed concept drift information of real-world datasets, like the start, the end of change and so on. We employ six widely used synthetic datasets SEA, CIR, SIN and STA with corresponding variants into experiments. Besides, another six synthetic datasets for binary classification are also adopted: 1CDT, 1CHT, UG-2C-2D, UG-2C-3D, UG-2C-5D, and GEARS-2C-2D. A brief statistics are summarized in Table 1. We provide the datasets information in Appendix E.

We plot the *holdout accuracy* comparisons over three synthetic datasets, SEA200A, SEA200G and SEA500G. Since some of compared approaches are batch style, following the splitting setting in Sun *et al.* [2018], we split them into 120 epochs to have a clear presentation. The holdout accuracy is calculated over testing data generated according to the identical distribution as training data at each time stamp. For SEA and its variants, the distribution changes for seven times. From Figure 2, we can see that all the approaches drop when an abrupt concept drift occurs. Nevertheless, our approach CONDOR is relatively stable and rises up rapidly with more data items coming, with the highest accuracy compared with other approaches, which validates its effectiveness.

Real-world Datasets. We adopt 10 real-world datasets: Usenet-1, Usenet-2, Luxembourg, Spam, Email, Weather, GasSensor, Powersupply, Electricity and Covertypes. The number of data

⁵Except for Covertypes and GasSensor datasets, we set $p = 200$, since Covertypes is extremely large with 581,012 data items in total and GasSensor is the multi-class dataset which has a higher sample complexity.

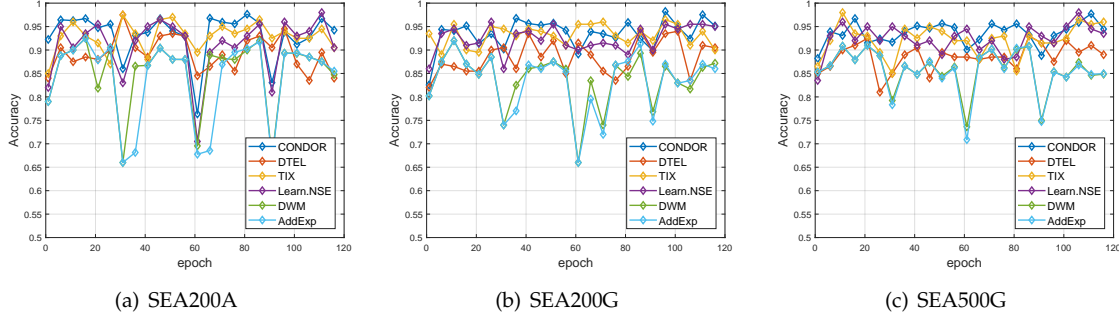


Figure 2: Holdout accuracy comparisons on three synthetic datasets.

Table 2: Performance comparisons on synthetic and real-world datasets. Besides, ● (○) indicates our approach CONDOR is significantly better (worse) than compared approaches (paired t -tests at 95% significance level).

Dataset	Ensemble Category			Model-Reuse Category		Ours CONDOR
	Learn ⁺⁺ .NSE	DWM	AddExp	DTEL	TIX	
SEA200A	84.48 ± 0.19 ●	86.07 ± 0.30 ●	84.35 ± 0.86 ●	80.50 ± 0.58 ●	82.79 ± 0.27 ●	86.67 ± 0.21
SEA200G	85.48 ± 0.33 ●	86.92 ± 0.13 ●	85.54 ± 0.69 ●	80.73 ± 0.19 ●	82.95 ± 0.12 ●	87.63 ± 0.24
SEA500G	86.03 ± 0.19 ●	87.63 ± 0.06 ●	87.14 ± 0.12 ●	80.42 ± 0.24 ●	83.26 ± 0.07 ●	88.21 ± 0.04
CIR500G	84.77 ± 0.56 ○	77.09 ± 0.71 ○	76.48 ± 0.81 ○	79.03 ± 0.34 ○	66.38 ± 0.85 ●	68.41 ± 0.87
SIN500G	79.41 ± 0.07 ○	66.99 ± 0.10 ○	66.81 ± 0.12 ○	74.93 ± 0.34 ○	62.73 ± 0.14 ●	65.68 ± 0.12
STA500G	83.97 ± 0.13 ●	87.43 ± 0.18 ●	86.89 ± 0.27 ●	88.26 ± 0.18 ●	85.95 ± 0.07 ●	88.60 ± 0.07
1CDT	99.77 ± 0.14 ●	99.92 ± 0.10	99.92 ± 0.10	99.69 ± 0.11 ●	99.56 ± 0.08 ●	99.95 ± 0.04
1CHT	99.69 ± 0.20	99.71 ± 0.28	99.56 ± 0.46	92.08 ± 0.22 ●	99.41 ± 0.22 ●	99.86 ± 0.13
UG-2C-2D	94.42 ± 0.12 ●	95.60 ± 0.12 ○	94.36 ± 0.78 ●	93.98 ± 0.13 ●	94.69 ± 0.13 ●	95.27 ± 0.09
UG-2C-3D	93.82 ± 0.60 ●	95.23 ± 0.59	94.61 ± 0.73 ●	92.94 ± 0.72 ●	94.31 ± 0.69 ●	94.84 ± 0.59
UG-2C-5D	90.30 ± 0.30 ●	92.85 ± 0.23 ○	92.20 ± 0.23 ○	88.21 ± 0.35 ●	89.84 ± 0.38 ●	91.83 ± 0.24
GEARS-2C-2D	95.82 ± 0.02 ●	95.83 ± 0.02 ●	95.83 ± 0.02 ●	94.96 ± 0.03 ●	95.03 ± 0.02 ●	95.91 ± 0.01
Usenet-1	63.76 ± 2.01 ●	67.26 ± 3.11 ●	62.11 ± 2.67 ●	68.02 ± 1.19 ●	65.03 ± 1.70 ●	73.13 ± 1.12
Usenet-2	72.42 ± 1.14 ●	68.41 ± 1.17 ●	70.55 ± 2.41 ●	72.02 ± 0.87 ●	70.56 ± 1.15 ●	75.13 ± 1.06
Luxembourg	98.64 ± 0.00 ●	90.42 ± 0.55 ●	90.77 ± 0.52 ●	100.0 ± 0.00	90.99 ± 0.97 ●	99.98 ± 0.03
Spam	90.79 ± 0.85 ●	92.18 ± 0.34 ●	91.78 ± 0.33 ●	85.53 ± 1.22 ●	87.10 ± 1.45 ●	95.22 ± 0.48
Email	74.21 ± 4.61 ●	72.58 ± 4.10 ●	60.78 ± 6.12 ●	83.36 ± 1.87 ●	79.83 ± 3.73 ●	91.60 ± 1.86
Weather	75.99 ± 0.36 ●	70.83 ± 0.49 ●	70.07 ± 0.34 ●	68.92 ± 0.27 ●	70.21 ± 0.33 ●	79.37 ± 0.26
GasSensor	42.36 ± 3.72 ●	76.61 ± 0.36 ●	76.61 ± 0.36 ●	63.82 ± 3.64 ●	43.40 ± 2.88 ●	81.57 ± 3.77
Powersupply	74.06 ± 0.28 ○	72.09 ± 0.29 ●	72.13 ± 0.23 ●	69.90 ± 0.38 ●	68.34 ± 0.16 ●	72.82 ± 0.29
Electricity	78.97 ± 0.18 ●	78.03 ± 0.17 ●	75.62 ± 0.42 ●	81.05 ± 0.35 ●	58.44 ± 0.71 ●	84.73 ± 0.33
Coverttype	79.08 ± 1.30 ●	74.17 ± 0.87 ●	73.13 ± 1.53 ●	69.43 ± 1.30 ●	64.60 ± 0.89 ●	89.58 ± 0.14
CONDOR w/t/1	18/ 1/ 3	14/ 3/ 4	17/ 2/ 3	19/ 1/ 2	22/ 0/ 0	rank first 16/ 22

items varies from 1,500 to 581,012, and the class number varies from 2 to 6. Detailed descriptions are provided in Appendix E.2. We conduct all the experiments for 10 trails and report overall mean and standard deviation of predictive accuracy in Table 2, synthetic datasets are also included. As we can see, CONDOR has a significant advantage over other comparisons. Actually, it achieves the best on 16 over 22 datasets in total. Besides, it ranks the second on four other datasets. The reason CONDOR behaves poor on CIR500G and SIN500G is that these two datasets are highly nonlinear (generated by a circle and sine function, respectively.). It is also noteworthy that CONDOR behaves significant better than other approaches in real-world datasets. These show the superiority of our proposed approach.

6 Conclusion

In this paper, a novel and effective approach CONDOR is proposed for handling concept drift via model reuse, which consists of two key components, ModelUpdate and WeightUpdate. Our approach is built on a drift detector, when a drift is detected or a maximum accumulation number is achieved, ModelUpdate leverages and reuses previous models in a weighted manner. Meanwhile, WeightUpdate adaptively adjusts weights of previous models according to their performance. By the generalization analysis, we prove that the model reuse strategy helps if we properly reuse previous models. Through regret analysis, we show that the weight concentrate on those better-fit models, and the approach achieves a fair dynamic cumulative regret. Empirical results show the superiority of our approach to other comparisons, on both synthetic and real-world datasets.

In the future, it would be interesting to incorporate more techniques from model reuse learning into handling concept drift problems.

References

- Peter L. Bartlett and Shahar Mendelson. Rademacher and gaussian complexities: Risk bounds and structural results. *Journal of Machine Learning Research*, 3:463–482, 2002.
- Alina Beygelzimer, Satyen Kale, and Haipeng Luo. Optimal and adaptive algorithms for online boosting. In *International Conference on Machine Learning, ICML*, pages 2323–2331, 2015.
- Albert Bifet and Ricard Gavaldà. Learning from time-changing data with adaptive windowing. In *Proceedings of the Seventh SIAM International Conference on Data Mining*, pages 443–448, 2007.
- Olivier Bousquet, Stéphane Boucheron, and Gábor Lugosi. Introduction to statistical learning theory. In *Advanced Lectures on Machine Learning, ML Summer Schools 2003*, pages 169–207, 2003.
- Olivier Bousquet. *Concentration inequalities and empirical processes theory applied to the analysis of learning algorithms*. PhD thesis, Ecole Polytechnique, 2002.
- Robert Catral, Franz Oppacher, and Dwight Deugo. Evolutionary data mining with automatic rule generalization. 2002.
- Nicolo Cesa-Bianchi and Gábor Lugosi. *Prediction, learning, and games*. Cambridge university press, 2006.
- Nicolò Cesa-Bianchi, Yoav Freund, David Haussler, David P. Helmbold, Robert E. Schapire, and Manfred K. Warmuth. How to use expert advice. *Journal of the ACM*, 44(3):427–485, 1997.
- Yanping Chen, Eamonn Keogh, Bing Hu, Nurjahan Begum, Anthony Bagnall, Abdullah Mueen, and Gustavo Batista. The ucr time series classification archive. 2015.
- Koby Crammer, Yishay Mansour, Eyal Even-Dar, and Jennifer Wortman Vaughan. Regret minimization with concept drift. In *Annual Conference Computational Learning Theory, COLT*, pages 168–180, 2010.
- Vinícius M. A. de Souza, Diego Furtado Silva, João Gama, and Gustavo E. A. P. A. Batista. Data stream classification guided by clustering on nonstationary environments and extreme verification latency. In *SIAM International Conference on Data Mining, SDM*, pages 873–881, 2015.

- Simon S. Du, Jayanth Koushik, Aarti Singh, and Barnabás Póczos. Hypothesis transfer learning via transformation functions. In *Advances in Neural Information Processing Systems, NIPS*, pages 574–584, 2017.
- Lixin Duan, Ivor W. Tsang, Dong Xu, and Tat-Seng Chua. Domain adaptation from multiple sources via auxiliary classifiers. In *International Conference on Machine Learning, ICML*, pages 289–296, 2009.
- Ryan Elwell and Robi Polikar. Incremental learning of concept drift in nonstationary environments. *IEEE Transactions on Neural Networks*, 22(10):1517–1531, 2011.
- George Forman. Tackling concept drift by temporal inductive transfer. In *International ACM SIGIR Conference on Research & Development in Information Retrieval, SIGIR*, pages 252–259, 2006.
- João Gama and Petr Kosina. Recurrent concepts in data streams classification. *Knowledge and Information Systems*, 40(3):489–507, 2014.
- João Gama, Ricardo Rocha, and Pedro Medas. Accurate decision trees for mining high-speed data streams. In *ACM SIGKDD International Conference on Knowledge Discovery & Data Mining, KDD*, pages 523–528, 2003.
- João Gama, Indre Zliobaite, Albert Bifet, Mykola Pechenizkiy, and Abdelhamid Bouchachia. A survey on concept drift adaptation. *ACM Computing Surveys*, 46(4):44:1–44:37, 2014.
- Heitor Murilo Gomes, Jean Paul Barddal, Fabrício Enembreck, and Albert Bifet. A survey on ensemble learning for data stream classification. *ACM Computing Surveys*, 50(2):23:1–23:36, 2017.
- Maayan Harel, Shie Mannor, Ran El-Yaniv, and Koby Crammer. Concept drift detection through resampling. In *International Conference on Machine Learning, ICML*, pages 1009–1017, 2014.
- Michael Harries and New South Wales. Splice-2 comparative evaluation: Electricity pricing. *Technical Report of South Wales University*, 1999.
- David P. Helmbold and Philip M. Long. Tracking drifting concepts by minimizing disagreements. *Machine Learning*, 14(1):27–45, 1994.
- Ghazal Jaber, Antoine Cornuéjols, and Philippe Tarroux. A new on-line learning method for coping with recurring concepts: The ADACC system. In *International Conference on Neural Information Processing, ICONIP*, pages 595–604, 2013.
- Sham M. Kakade, Shai Shalev-Shwartz, and Ambuj Tewari. Regularization techniques for learning with matrices. *Journal of Machine Learning Research*, 13:1865–1890, 2012.
- Ioannis Katakis, Grigorios Tsoumakas, and Ioannis P. Vlahavas. An ensemble of classifiers for coping with recurring contexts in data streams. In *European Conference on Artificial Intelligence, ECAI*, pages 763–764, 2008.
- Ioannis Katakis, Grigorios Tsoumakas, Evangelos Banos, Nick Bassiliades, and Ioannis P. Vlahavas. An adaptive personalized news dissemination system. *Journal of Intelligent Information Systems*, 32(2):191–212, 2009.
- Ioannis Katakis, Grigorios Tsoumakas, and Ioannis P. Vlahavas. Tracking recurring contexts using ensemble classifiers: an application to email filtering. *Knowledge and Information Systems*, 22(3):371–391, 2010.

- Ralf Klittenberg and Thorsten Joachims. Detecting concept drift with support vector machines. In *International Conference on Machine Learning, ICML*, pages 487–494, 2000.
- Ralf Klittenberg. Learning drifting concepts: Example selection vs. example weighting. *Intelligent Data Analysis*, 8(3):281–300, 2004.
- Jeremy Z. Kolter and Marcus A. Maloof. Dynamic weighted majority: A new ensemble method for tracking concept drift. In *IEEE International Conference on Data Mining, ICDM*, pages 123–130, 2003.
- Jeremy Z. Kolter and Marcus A. Maloof. Using additive expert ensembles to cope with concept drift. In *International Conference on Machine Learning, ICML*, pages 449–456, 2005.
- J. Zico Kolter and Marcus A. Maloof. Dynamic weighted majority: An ensemble method for drifting concepts. *Journal of Machine Learning Research*, 8:2755–2790, 2007.
- Ivan Koychev. Gradual forgetting for adaptation to concept drift. In *In Proceedings of ECAI 2000 Workshop Current Issues in Spatio-Temporal Reasoning*, pages 101–106, 2000.
- Ludmila I. Kuncheva and Indre Zliobaite. On the window size for classification in changing environments. *Intelligent Data Analysis*, 13(6):861–872, 2009.
- Ilya Kuzborskij and Francesco Orabona. Stability and hypothesis transfer learning. In *International Conference on Machine Learning, ICML*, pages 942–950, 2013.
- Ilya Kuzborskij and Francesco Orabona. Fast rates by transferring from auxiliary hypotheses. *Machine Learning*, 106(2):171–195, 2017.
- Michel Ledoux and Michel Talagrand. *Probability in Banach Spaces: isoperimetry and processes*. Springer Science & Business Media, 2013.
- Yunwen Lei, Ürün Dogan, Alexander Binder, and Marius Kloft. Multi-class svms: From tighter data-dependent generalization bounds to novel algorithms. In *Advances in Neural Information Processing Systems, NIPS*, pages 2035–2043, 2015.
- Nan Li, Ivor W. Tsang, and Zhi-Hua Zhou. Efficient optimization of performance measures by classifier adaptation. *IEEE Transactions on Pattern Analysis and Machine Intelligence*, 35(6):1370–1382, 2013.
- Andreas Maurer. A vector-contraction inequality for rademacher complexities. In *International Conference on Algorithmic Learning Theory, ALT*, pages 3–17, 2016.
- Mehryar Mohri and Andres Muñoz Medina. New analysis and algorithm for learning with drifting distributions. In *ALT*, pages 124–138, 2012.
- Mehryar Mohri, Afshin Rostamizadeh, and Ameet Talwalkar. *Foundations of machine learning*. MIT press, 2012.
- Robert E. Schapire and Yoav Freund. *Boosting: Foundations and Algorithms*. The MIT Press, 2012.
- Robert E. Schapire. The strength of weak learnability. *Machine Learning*, 5:197–227, 1990.
- Jeffrey C. Schlimmer and Richard H. Granger. Incremental learning from noisy data. *Machine Learning*, 1(3):317–354, 1986.

- Bernhard Schölkopf, Ralf Herbrich, and Alexander J. Smola. A generalized representer theorem. In *Annual Conference Computational Learning Theory, COLT*, pages 416–426, 2001.
- Noam Segev, Maayan Harel, Shie Mannor, Koby Crammer, and Ran El-Yaniv. Learn on source, refine on target: A model transfer learning framework with random forests. *IEEE Transactions on Pattern Analysis and Machine Intelligence*, 39(9):1811–1824, 2017.
- Nathan Srebro, Karthik Sridharan, and Ambuj Tewari. Smoothness, low noise and fast rates. In *Advances in Neural Information Processing Systems, NIPS*, pages 2199–2207. 2010.
- W. Nick Street and YongSeog Kim. A streaming ensemble algorithm (SEA) for large-scale classification. In *ACM SIGKDD International Conference on Knowledge Discovery & Data Mining, KDD*, pages 377–382, 2001.
- Y. Sun, K. Tang, Z. Zhu, and X. Yao. Concept drift adaptation by exploiting historical knowledge. *IEEE Transactions on Neural Networks and Learning Systems*, To appear, 2018.
- Johan AK Suykens, Tony Van Gestel, and Jos De Brabanter. *Least squares support vector machines*. World Scientific, 2002.
- Tatiana Tommasi, Francesco Orabona, and Barbara Caputo. Safety in numbers: Learning categories from few examples with multi model knowledge transfer. In *IEEE Conference on Computer Vision and Pattern Recognition, CVPR*, pages 3081–3088, 2010.
- Tatiana Tommasi, Francesco Orabona, and Barbara Caputo. Learning categories from few examples with multi model knowledge transfer. *IEEE Transactions on Pattern Analysis and Machine Intelligence*, 36(5):928–941, 2014.
- Alexander Vergara, Shankar Vembu, Tuba Ayhan, Margaret A Ryan, Margie L Homer, and Ramón Huerta. Chemical gas sensor drift compensation using classifier ensembles. *Sensors and Actuators B: Chemical*, 166:320–329, 2012.
- Michail Vlachos, Carlotta Domeniconi, Dimitrios Gunopulos, George Kollios, and Nick Koudas. Non-linear dimensionality reduction techniques for classification and visualization. In *ACM SIGKDD International Conference on Knowledge Discovery & Data Mining, KDD*, pages 645–651, 2002.
- Zhi-Hua Zhou. *Ensemble Methods: Foundations and Algorithms*. Chapman & Hall/CRC Press, 2012.
- Martin Zinkevich. Online convex programming and generalized infinitesimal gradient ascent. In *International Conference on Machine Learning, ICML*, pages 928–936, 2003.
- Indre Zliobaite. Combining similarity in time and space for training set formation under concept drift. *Intelligent Data Analysis*, 15(4):589–611, 2011.

Appendix A Prerequisite Knowledge and Technical Lemmas

In this section, we introduce prerequisite knowledge for proving main results technical lemmas. Specifically, we will utilize Rademacher complexity [Bartlett and Mendelson, 2002] in proving generalization bounds. Besides, we will also exploit the function properties when bounding Rademacher complexity and proving the regret bounds.

A.1 Rademacher Complexity

To simplify the presentation, first, we introduce some notations. Let S be a sample of m points drawn i.i.d. according to distribution \mathcal{D} , then the risk and empirical risk of hypothesis h are defined by

$$R(h) = \mathbb{E}_{(\mathbf{x}, y) \sim \mathcal{D}} [\ell(h(\mathbf{x}), y)], \quad \hat{R}_S(h) = \frac{1}{m} \sum_{i=1}^m \ell(h(\mathbf{x}_i), y_i).$$

In the following, we will utilize the notion of Rademacher complexity [Bartlett and Mendelson, 2002] to measure the hypothesis complexity and use it to bound the generalization error.

Definition 2. (*Rademacher Complexity [Bartlett and Mendelson, 2002]*) Let \mathcal{G} be a family of functions and a fixed sample of size m as $S = (\mathbf{z}_1, \dots, \mathbf{z}_m)$. Then, the *empirical Rademacher complexity* of \mathcal{G} with respect to the sample S is defined as:

$$\hat{\mathfrak{R}}_S(\mathcal{G}) = \mathbb{E}_\sigma \left[\sup_{g \in \mathcal{G}} \frac{1}{m} \sum_{i=1}^m \sigma_i g(\mathbf{z}_i) \right].$$

Besides, the *Rademacher complexity* of \mathcal{G} is the expectation of the empirical Rademacher complexity over all samples of size m drawn according to \mathcal{D} :

$$\mathfrak{R}_m(\mathcal{G}) = \mathbb{E}_{S \sim \mathcal{D}^m} [\hat{\mathfrak{R}}_S(\mathcal{G})]. \quad (12)$$

A.2 Function Properties

In this paragraph, we introduce several common and useful functional properties.

Definition 3 (Lipschitz Continuity). A function $f : \mathcal{K} \rightarrow \mathbb{R}$ is L -Lipschitz continuous w.r.t. a norm $\|\cdot\|$ over domain \mathcal{K} if for all $\mathbf{x}, y \in \mathcal{K}$, we have

$$|f(y) - f(\mathbf{x})| \leq L \|y - \mathbf{x}\|.$$

Definition 4 (Strong Convexity). A function $f : \mathcal{K} \rightarrow \mathbb{R}$ is λ -strongly convex w.r.t. a norm $\|\cdot\|$ if for all $\mathbf{x}, y \in \mathcal{K}$ and for any $\alpha \in [0, 1]$, we have

$$f((1 - \alpha)\mathbf{x} + \alpha y) \leq (1 - \alpha)f(\mathbf{x}) + \alpha f(y) - \frac{\lambda}{2} \alpha(1 - \alpha) \|\mathbf{x} - y\|^2.$$

A common and equivalent form for differentiable case is,

$$f(y) \geq f(\mathbf{x}) + \nabla f(\mathbf{x})^\top (y - \mathbf{x}) + \frac{\lambda}{2} \|y - \mathbf{x}\|^2. \quad (13)$$

Definition 5 (Smoothness). A function $f : \mathcal{K} \rightarrow \mathbb{R}$ is σ -smooth w.r.t. a norm $\|\cdot\|$ if for all $\mathbf{x}, y \in \mathcal{K}$, we have

$$f(y) \leq f(\mathbf{x}) + \nabla f(\mathbf{x})^\top (y - \mathbf{x}) + \frac{\sigma}{2} \|y - \mathbf{x}\|^2.$$

If f is differentiable, the above condition is equivalent to a Lipschitz condition over the gradients,

$$\|\nabla f(\mathbf{x}) - \nabla f(y)\| \leq \sigma \|\mathbf{x} - y\|.$$

A.3 Technical Lemmas

To obtain a fast generalization rate, essentially, we need a Bernstein-type concentration inequality. And we adopt the functional generalization of Bennett's inequality due to Bousquet [Bousquet, 2002], for self-containedness, we state the conclusion in Lemma 2 as follow.

Lemma 2 (Theorem 2.11 in Bousquet [2002]). Assume the X_i are identically distributed according to P . Let \mathcal{F} be a countable set of functions from \mathcal{X} to \mathbb{R} and assume that all functions f in \mathcal{F} are P -measurable, square-integrable and satisfy $\mathbb{E}[f] = 0$. If $\sup_{f \in \mathcal{F}} \text{ess sup } f \leq 1$ then we denote

$$Z = \sup_{f \in \mathcal{F}} \sum_{i=1}^n f(X_i),$$

and if $\sup_{f \in \mathcal{F}} \|f\|_\infty \leq 1$, Z can be defined as above or as

$$Z = \sup_{f \in \mathcal{F}} \left| \sum_{i=1}^n f(X_i) \right|.$$

Let σ be a positive real number such that $\sigma^2 \geq \sup_{f \in \mathcal{F}} \text{Var}[f(X_1)]$ almost surely, then for all $x \geq 0$, we have

$$\Pr [Z \geq \mathbb{E}[Z] + t] \leq \exp \left\{ -v g \left(\frac{t}{v} \right) \right\},$$

with $v = n\sigma^2 + 2\mathbb{E}[Z]$ and $g(y) = (1+y) \log(1+y) - y$, also

$$\Pr \left[Z \geq \mathbb{E}[Z] + \sqrt{2tv} + \frac{t}{3} \right] \leq e^{-t}.$$

Besides, for a strongly convex regularizer, we have following property, which will be useful in proving Theorem 1.

Lemma 3 (Corollary 4 in Kakade *et al.* [2012]). If Ω is λ -strongly convex w.r.t. a norm $\|\cdot\|$ and $\Omega^*(\mathbf{0}) = 0$, then, denoting the partial sum $\sum_{j \leq i} \mathbf{v}_j$ by $\mathbf{v}_{1:i}$, we have for any sequence $\mathbf{v}_1, \dots, \mathbf{v}_n$ and for any \mathbf{u} ,

$$\sum_{i=1}^n \langle \mathbf{v}_i, \mathbf{u} \rangle \leq f^*(\mathbf{v}_{1:n}) \leq \sum_{i=1}^n \langle \nabla f^*(\mathbf{v}_{1:i-1}), \mathbf{v}_i \rangle + \frac{1}{2\beta} \sum_{i=1}^n \|\mathbf{v}_i\|_*^2.$$

Lemma 4 (Lemma 8.1 in Mohri *et al.* [2012]). Let $\mathcal{F}_1, \dots, \mathcal{F}_l$ be l hypothesis sets in $\mathbb{R}^{\mathcal{X}}$, $l \geq 1$, and let $\mathcal{G} = \{\max\{h_1, \dots, h_l\} : h_i \in \mathcal{F}_i, i \in [1, l]\}$. Then, for any sample S of size m , the empirical Rademacher complexity of \mathcal{G} can be upper bounded as follows:

$$\hat{\mathfrak{R}}_S(\mathcal{G}) \leq \sum_{j=1}^l \hat{\mathfrak{R}}_S(\mathcal{F}_j).$$

Proof. The proof is based on two observations on max operator. First one is that $\max\{h_1, \dots, h_l\} = \max\{h_1, \max\{h_2, \dots, h_l\}\}$, and thus we can focus on the case when $l = 2$. The second observation is that for any $h_1 \in \mathcal{F}_1$ and $h_2 \in \mathcal{F}_2$, we have

$$\max\{h_1, h_2\} = \frac{1}{2} [h_1 + h_2 + |h_1 - h_2|].$$

One can refer to page 186 in Mohri *et al.* [2012] for details. □

Appendix B Proof of Theorem 1

We prove the statement in Theorem 1 in the following two steps,

- (1) First, in Lemma 5, we establish fast generalization error bound in terms of the Rademacher complexity of loss function family, i.e., $\mathfrak{R}_m(\mathcal{L})$.
- (2) Next, in Lemma 6, we upper bound the Rademacher complexity of Lipschitz loss function family by terms regarding to R_p , which is defined as the risk of the combination of previous models h_p on current distribution \mathcal{D}_k .

B.1 Fast Rate Generalization Error Bound

Lemma 5. Assume that the non-negative loss function $\ell : \mathcal{Y} \times \mathcal{Y} \rightarrow \mathbb{R}_+$ is bounded by $M \geq 0$. Let \mathcal{H} denote the hypothesis set and S be a sample of m points drawn i.i.d. according to distribution \mathcal{D} . For any constant $r \geq 0$, define the loss function family \mathcal{L} as

$$\mathcal{L} = \{(\mathbf{x}, y) \rightarrow \ell(h(\mathbf{x}), y) : h \in \mathcal{H} \wedge R(h) \leq r\}.$$

Then, for any $\delta > 0$, with probability at least $1 - \delta$, the following holds for all $h \in \mathcal{H}_r$ with $\mathcal{H}_r = \{h : h \in \mathcal{H} \wedge R(h) \leq r\}$,

$$R(h) - \hat{R}_S(h) \leq 2\mathfrak{R}_m(\mathcal{L}) + \frac{3M \log(1/\delta)}{4m} + 3\sqrt{\frac{(8\mathfrak{R}_m(\mathcal{L}) + r)M \log(1/\delta)}{4m}}. \quad (14)$$

Proof. The proof is based on the application of functional generalization of Bennett's inequality due to Bousquet [Bousquet, 2002].

For any sample $S = \{(\mathbf{x}_1, y_1), \dots, (\mathbf{x}_m, y_m)\}$ and any $h \in \mathcal{H}_r$, we turn to consider the uniform upper bound of $R(h) - \hat{R}_S(h)$. The proof consists of applying functional generalization of Bennett's inequality to function Φ defined for any sample S by

$$\Phi_S = \frac{m}{2M} \sup_{h \in \mathcal{H}_r} \{R(h) - \hat{R}_S(h)\},$$

which satisfies the condition in Lemma 2, that is, $\sup_{h \in \mathcal{H}_r} \text{ess sup}_{\frac{1}{2M}} (\mathbb{E}[\ell(h(\mathbf{x}), y)] - \ell(h(\mathbf{x}_i), y_i)) \leq 1$, due to the boundedness of loss function. Now, we can apply Lemma 2,

$$\Pr[\Phi_S \geq \mathbb{E}_S[\Phi_S] + t] \leq \exp\left\{-vg\left(\frac{t}{v}\right)\right\},$$

where

$$v = m\sigma^2 + 2\mathbb{E}_S[\Phi_S],$$

$$\sigma^2 = \sup_{h \in \mathcal{H}_r} \text{Var}\left[\frac{1}{2M} \mathbb{E}_{(\mathbf{x}', y) \sim \mathcal{D}}[\ell(h(\mathbf{x}'), y')] - \ell(h(\mathbf{x}), y)\right].$$

And we can reverse the above inequality and obtain that for any $\delta > 0$, with probability at least $1 - \delta$, the following holds for all $h \in \mathcal{H}_r$,

$$\Phi_S \leq \mathbb{E}_S[\Phi_S] + \frac{3 \log(1/\delta)}{4} + \frac{3}{2} \sqrt{v \log(1/\delta)}. \quad (15)$$

Thus, we proceed to bound term σ^2 and $\mathbb{E}_S[\Phi_S]$. First, we bound the term σ^2 .

$$\begin{aligned}
\sigma^2 &= \sup_{h \in \mathcal{H}_r} \text{Var} \left[\frac{1}{2M} \mathbb{E}_{(\mathbf{x}', y') \sim \mathcal{D}} [\ell(h(\mathbf{x}'), y')] - \ell(h(\mathbf{x}), y) \right] \\
&= \sup_{h \in \mathcal{H}_r} \mathbb{E}_{(\mathbf{x}, y) \sim \mathcal{D}} \left[\frac{1}{4M^2} \left(\ell(h(\mathbf{x}), y) - \mathbb{E}_{(\mathbf{x}', y') \sim \mathcal{D}} [\ell(h(\mathbf{x}'), y')] \right)^2 \right] \\
&\leq \sup_{h \in \mathcal{H}_r} \frac{1}{4M^2} \mathbb{E}_{(\mathbf{x}, y) \sim \mathcal{D}} [\ell(h(\mathbf{x}), y)^2] \\
&\leq \sup_{h \in \mathcal{H}_r} \frac{1}{4M} \mathbb{E}_{(\mathbf{x}, y) \sim \mathcal{D}} [\ell(h(\mathbf{x}), y)] \tag{16}
\end{aligned}$$

$$= \sup_{h \in \mathcal{H}_r} \frac{1}{4M} R(h) = \frac{r}{4M}. \tag{17}$$

Eq. (16) holds due to the boundedness of loss function, and Eq. (17) holds because of the definition of \mathcal{H}_r , as we know $R(h) \leq r$ holds for all $h \in \mathcal{H}_r$.

Next, we turn to prove the bound on $\mathbb{E}_S[\Phi_S]$ by utilizing the standard *symmetrization* technique [Bousquet *et al.*, 2003; Mohri *et al.*, 2012].

$$\begin{aligned}
\mathbb{E}_S[\Phi_S] &= \mathbb{E}_S \left[\frac{m}{2M} \sup_{h \in \mathcal{H}_r} \{R(h) - \hat{R}_S(h)\} \right] \\
&= \mathbb{E}_S \left[\frac{m}{2M} \sup_{h \in \mathcal{H}_r} \{\mathbb{E}_{S'}[\hat{R}_{S'}(h) - \hat{R}_S(h)]\} \right] \\
&\leq \frac{m}{2M} \mathbb{E}_{S, S'} \left[\sup_{h \in \mathcal{H}_r} \{\hat{R}_{S'}(h) - \hat{R}_S(h)\} \right] \tag{18}
\end{aligned}$$

$$\begin{aligned}
&= \frac{m}{2M} \mathbb{E}_{S, S'} \left[\sup_{h \in \mathcal{H}_r} \frac{1}{m} \sum_{i=1}^m (\ell(h(\mathbf{x}'_i), y'_i) - \ell(h(\mathbf{x}_i), y_i)) \right] \\
&= \frac{m}{2M} \mathbb{E}_{\sigma, S, S'} \left[\sup_{h \in \mathcal{H}_r} \frac{1}{m} \sum_{i=1}^m \sigma_i (\ell(h(\mathbf{x}'_i), y'_i) - \ell(h(\mathbf{x}_i), y_i)) \right] \tag{19}
\end{aligned}$$

$$\leq \frac{m}{2M} \mathbb{E}_{\sigma, S'} \left[\sup_{h \in \mathcal{H}_r} \frac{1}{m} \sum_{i=1}^m \sigma_i (\ell(h(\mathbf{x}'_i), y'_i)) \right] + \frac{m}{2M} \mathbb{E}_{\sigma, S} \left[\sup_{h \in \mathcal{H}_r} \frac{1}{m} \sum_{i=1}^m -\sigma_i (\ell(h(\mathbf{x}_i), y_i)) \right] \tag{20}$$

$$= \frac{m}{M} \mathbb{E}_{\sigma, S} \left[\sup_{h \in \mathcal{H}_r} \frac{1}{m} \sum_{i=1}^m \sigma_i (\ell(h(\mathbf{x}_i), y_i)) \right] = \frac{m}{M} \mathfrak{R}_m(\mathcal{L}).$$

(18) holds due to the convexity of supremum function, and thus we can apply Jensen's inequality. In (19), we introduce Rademacher random variables σ_1 s, that are uniformly distributed independent random variables taking values in $\{-1, +1\}$, and thus this does not change the expectation. (19) holds due to the sub-additivity of supremum function.

Thus, we can obtain the bound on v ,

$$v = m\sigma^2 + 2\mathbb{E}_S[\Phi_S] \leq \frac{rm}{4M} + \frac{2m}{M} \mathfrak{R}_m(\mathcal{L}).$$

Combining the bounds on v and $\mathbb{E}_S[\Phi_S]$, we have

$$\begin{aligned}\Phi_S &= \frac{m}{2M} \sup_{h \in \mathcal{H}_r} \{R(h) - \hat{R}_S(h)\} \\ &\leq \frac{m}{M} \mathfrak{R}_m(\mathcal{L}) + \frac{3 \log(1/\delta)}{4} + \frac{3}{2} \sqrt{\left(\frac{rm}{4M} + \frac{2m}{M} \mathfrak{R}_m(\mathcal{L})\right) \log(1/\delta)}.\end{aligned}$$

Hence, we complete the proof that for any hypothesis $h \in \mathcal{H}_r$, we have

$$\begin{aligned}R(h) - \hat{R}_S(h) &\leq \sup_{h \in \mathcal{H}_r} \{R(h) - \hat{R}_S(h)\} = (2M/m)\Phi_S \\ &\leq 2\mathfrak{R}_m(\mathcal{L}) + \frac{3M \log(1/\delta)}{4m} + 3\sqrt{\frac{(r + 8\mathfrak{R}_m(\mathcal{L}))M \log(1/\delta)}{4m}}.\end{aligned}$$

□

B.2 Rademacher Complexity of Lipschitz Loss Function Family

Lemma 6. Assume that the non-negative loss function $\ell : \mathcal{Y} \times \mathcal{Y} \rightarrow \mathbb{R}_+$ is bounded by $M \geq 0$, and is L -Lipschitz continuous. Given the model pool $\{h_1, h_2, \dots, h_p\}$ with $\mathbf{h}_p(\mathbf{x}) := [h_1(\mathbf{x}), h_2(\mathbf{x}), \dots, h_p(\mathbf{x})]^\top$, and h_p is a linear combination of previous models, i.e., $h_p(\mathbf{x}) = \langle \boldsymbol{\beta}, \mathbf{f}(\mathbf{x}) \rangle$. Define the feasible set $\mathcal{W} = \{\mathbf{w} : \Omega(\mathbf{w}) \leq \alpha \hat{R}_S(h_p)\}$ and $\mathcal{V} = \{\boldsymbol{\beta} : \Omega(\boldsymbol{\beta}) \leq \rho\}$, and let the loss function family \mathcal{L} be as,

$$\mathcal{L} = \{(\mathbf{x}, y) \rightarrow \ell(\langle \mathbf{w}, \mathbf{x} \rangle + h_p(\mathbf{x}), y) : \mathbf{w} \in \mathcal{W} \wedge \boldsymbol{\beta} \in \mathcal{V}\},$$

and let S be a sample of m points drawn i.i.d. according to distribution \mathcal{D} , then we have

$$\mathfrak{R}_m(\mathcal{L}) \leq 2L \sqrt{\frac{B^2 \alpha R_p + C^2 \rho}{\lambda m}}. \quad (21)$$

where $R_p = R(h_p)$, $B = \sup_{\mathbf{x} \in \mathcal{X}} \|\mathbf{x}\|_*$ and $C = \sup_{\mathbf{x} \in \mathcal{X}} \|\mathbf{h}_p(\mathbf{x})\|_*$.

Proof. Let \mathcal{L} be the loss function family associated with the hypothesis set \mathcal{H} . Namely, $\mathcal{L} = \{(\mathbf{x}, y) \rightarrow \ell(h(\mathbf{x}), y) : h \in \mathcal{H}\}$, where $\mathcal{H} = \{h_{\mathbf{w}, \boldsymbol{\beta}} : \mathbf{w} \in \mathcal{W} \wedge \boldsymbol{\beta} \in \mathcal{V}\}$. The empirical Rademacher complexity of \mathcal{L} is,

$$\begin{aligned}\hat{\mathfrak{R}}_S(\mathcal{L}) &= \frac{1}{m} \mathbb{E}_\sigma \left[\sup_{h \in \mathcal{H}} \sum_{i=1}^m \sigma_i \ell(h(\mathbf{x}_i), y_i) \right] \\ &= \frac{1}{m} \mathbb{E}_\sigma \left[\sup_{\mathbf{w} \in \mathcal{W}} \sum_{i=1}^m \sigma_i \ell(\langle \mathbf{w}, \mathbf{x}_i \rangle + h_p(\mathbf{x}_i), y_i) \right] \\ &\leq \frac{L}{m} \mathbb{E}_\sigma \left[\sup_{\mathbf{w} \in \mathcal{W}} \sum_{i=1}^m \sigma_i \langle \mathbf{w}, \mathbf{x}_i \rangle \right] + \frac{L}{m} \mathbb{E}_\sigma \left[\sup_{\boldsymbol{\beta} \in \mathcal{V}} \sum_{i=1}^m \sigma_i \langle \boldsymbol{\beta}, \mathbf{h}_p(\mathbf{x}_i) \rangle \right]\end{aligned} \quad (22)$$

The last inequality holds due to the fact that loss function ℓ is a L -Lipschitz continuous, and thus we can apply the *Talagrand's Comparison Inequality* [Ledoux and Talagrand, 2013] to relate the Rademacher complexity of loss function family and that of hypothesis set.

We turn to bound the two empirical Rademacher complexity terms in the r.h.s. of above inequality. Similar to the technique in Kakade *et al.* [2012], we utilize the primal-dual property of strongly-convex regularizer, and introduce the variable t_1 and t_2 into two Rademacher complexity terms separately, with aim to obtain a tighter bound by tuning the variables.

For the first term in the r.h.s. of (22), we apply Lemma 3 with $\mathbf{u} = \mathbf{w}$ and $\mathbf{v}_i = t_1 \mathbf{x}_i$,

$$\begin{aligned} & \mathbb{E}_\sigma \left[\sup_{\mathbf{w} \in \mathcal{W}} \frac{1}{m} \sum_{i=1}^m \langle \mathbf{w}, t_1 \sigma_i \mathbf{x}_i \rangle \right] \\ & \leq \frac{1}{m} \mathbb{E}_\sigma \left[\frac{t_1^2}{2\lambda} \sum_{i=1}^m \|\sigma_i \mathbf{x}_i\|_*^2 + \sup_{\mathbf{w} \in \mathcal{W}} \Omega(\mathbf{w}) + \sum_{i=1}^m \langle \nabla \Omega^*(\mathbf{v}_{1:i-1}), \sigma_i \mathbf{x}_i \rangle \right] \\ & \leq \frac{B^2 t_1^2}{2\lambda} + \frac{\alpha \hat{R}_S(h_p)}{m}, \end{aligned}$$

where the last inequality holds due to the fact that $\sup_{\mathbf{w} \in \mathcal{W}} \Omega(\mathbf{w}) \leq \alpha \hat{R}_S(h_p)$ and $\sup_{\mathbf{x} \in \mathcal{X}} \|\mathbf{x}\|_* \leq B$. By dividing t_1 on both sides, and notice that the above upper bound holds for any $t_1 > 0$, we choose a particular t_1 making the upper bound tight,

$$\frac{L}{m} \mathbb{E}_\sigma \left[\sup_{\mathbf{w} \in \mathcal{W}} \sum_{i=1}^m \sigma_i \langle \mathbf{w}, \mathbf{x}_i \rangle \right] \leq \inf_{t_1 > 0} L \left(\frac{B^2 t_1}{2\lambda} + \frac{\alpha \hat{R}_S(h_p)}{m t_1} \right) = L \sqrt{\frac{2B^2 \alpha \hat{R}_S(h_p)}{\lambda m}}. \quad (23)$$

Similarly, we introduce variable t_2 as tuning parameter for the second term in the r.h.s. of (22) with $\mathbf{u} = \mathbf{w}$ and $\mathbf{v}_i = t_2 \mathbf{h}_p(\mathbf{x}_i)$,

$$\begin{aligned} & \mathbb{E}_\sigma \left[\sup_{\beta \in \mathcal{V}} \frac{1}{m} \sum_{i=1}^m \langle \beta, t_2 \sigma_i \mathbf{h}_p(\mathbf{x}_i) \rangle \right] \\ & \leq \frac{1}{m} \mathbb{E}_\sigma \left[\frac{t_2^2}{2\lambda} \sum_{i=1}^m \|\sigma_i \mathbf{h}_p(\mathbf{x}_i)\|_*^2 + \sup_{\beta \in \mathcal{V}} \Omega(\beta) + \sum_{i=1}^m \langle \nabla \Omega^*(\mathbf{v}_{1:i-1}), \sigma_i \mathbf{h}_p(\mathbf{x}_i) \rangle \right] \\ & \leq \frac{t_2^2 C^2}{2\lambda} + \frac{\rho}{m}, \end{aligned}$$

where the last inequality holds due to the fact that $\sup_{\beta \in \mathcal{V}} \Omega(\beta) \leq \rho$ and $\sup_{\mathbf{x} \in \mathcal{X}} \|\mathbf{h}_p(\mathbf{x})\|_* \leq C$. By dividing t_2 on both sides, and notice that the above upper bound holds for any $t_2 > 0$, we choose a particular t_2 making the upper bound tight,

$$\frac{L}{m} \mathbb{E}_\sigma \left[\sup_{\beta \in \mathcal{V}} \sum_{i=1}^m \sigma_i \langle \beta, \mathbf{h}_p(\mathbf{x}_i) \rangle \right] \leq \inf_{t_2 > 0} L \left(\frac{t_2 C^2}{2\lambda} + \frac{\rho}{m t_2} \right) = L \sqrt{\frac{2C^2 \rho}{\lambda m}}. \quad (24)$$

Combing (23) and (24), we obtain the bound for $\hat{\mathfrak{R}}_S(\mathcal{L})$. Notice that the square-root function is concave, by applying the Jensen's inequality w.r.t. the both side, we have

$$\begin{aligned} \mathfrak{R}_m(\mathcal{L}) &= \mathbb{E}_S[\hat{\mathfrak{R}}_S(\mathcal{L})] \leq L \mathbb{E}_S \left[\sqrt{\frac{2B^2 \alpha \hat{R}_S(h_p)}{\lambda m}} + \sqrt{\frac{2C^2 \rho}{\lambda m}} \right] \\ &\leq L \left(\sqrt{\frac{2B^2 \alpha \mathbb{E}_S[\hat{R}_S(h_p)]}{\lambda m}} + \sqrt{\frac{2C^2 \rho}{\lambda m}} \right) \\ &= L \left(\sqrt{\frac{2B^2 \alpha R(h_p)}{\lambda m}} + \sqrt{\frac{2C^2 \rho}{\lambda m}} \right) \\ &\leq 2L \sqrt{\frac{B^2 \alpha R_p + C^2 \rho}{\lambda m}} \end{aligned}$$

The last inequality holds due to the fact that $\sqrt{a} + \sqrt{b} \leq \sqrt{2(a+b)}$, for any $a, b \geq 0$. Besides, R_p is short for $R(h_p)$. Hence, we complete the proof of the statement. \square

B.3 Proof of Theorem 1

Proof. To prove the generalization bound stated in Theorem 1, we turn to prove the uniform bound over the following hypothesis set

$$\mathcal{H} = \{\mathbf{x} \rightarrow \langle \mathbf{w}, \mathbf{x} \rangle + h_p(\mathbf{x}) : \Omega(\mathbf{w}) \leq \frac{1}{\lambda} \hat{R}(h_p) \wedge \hat{R}(h_{\mathbf{w},p}) \leq \hat{R}(h_p)\},$$

where $h_{\mathbf{w},p}(\mathbf{x}) = \langle \mathbf{w}, \mathbf{x} \rangle + h_p(\mathbf{x})$.

First, we verify that the model \hat{h}_S returned by ModelUpdate procedure belongs to the set \mathcal{H} . Since $\hat{\mathbf{w}}$ is optimal solution, it is apparently better than the choice $\mathbf{0}$,

$$\hat{R}_S(\hat{h}_S) + \lambda \Omega(\hat{\mathbf{w}}) \leq \hat{R}_S(h_p) + \lambda \Omega(\mathbf{0}) = \hat{R}_S(h_p),$$

combining the non-negative property of loss and regularizer, we know that \hat{h}_S belongs to the \mathcal{H} .

Besides, we can upper bound the Rademacher complexity of any hypothesis in the hypothesis set \mathcal{H} as,

$$r = \sup_{h \in \mathcal{H}} R(h) = \sup_{h \in \mathcal{H}} \mathbb{E}_S[\hat{R}_S(h)] \leq \mathbb{E}_S[\sup_{h \in \mathcal{H}} \hat{R}_S(h)] \leq \mathbb{E}_S[\hat{R}_S(h_p)] = R_p. \quad (25)$$

Thus, we can apply Lemma 5 by setting $r = R_p$, obtaining that for any $\delta > 0$, with probability at least $1 - \delta$, the following holds for all $h \in \mathcal{H}$,

$$R(h) - \hat{R}_S(h) \leq 2\mathfrak{R}_m(\mathcal{L}) + \frac{3M \log(1/\delta)}{4m} + 3\sqrt{\frac{(8\mathfrak{R}_m(\mathcal{L}) + R_p)M \log(1/\delta)}{4m}}. \quad (26)$$

To bound the Rademacher complexity term $\mathfrak{R}_m(\mathcal{L})$, we can apply Lemma 6 by setting $\alpha = 1/\lambda$,

$$\mathfrak{R}_m(\mathcal{L}) \leq 2L\sqrt{\frac{B^2 R_p + C^2 \lambda \rho}{\lambda^2 m}}.$$

This in conjunction with (26) yields (1). \square

Corollary 1. If further suppose an H -smooth condition on loss function, and under the same conditions (except L -Lipschitz continuity) stated in Theorem 1. Then, for any $\delta > 0$, with probability at least $1 - \delta$, the following holds,

$$R(h_k) - \hat{R}(h_k) = O\left(\frac{1}{\sqrt{m}} \left(\sqrt{R_p} + \sqrt{\frac{\sqrt{H} R_p}{\lambda^2}} + \sqrt[4]{\frac{\sqrt{H} R_p}{\lambda^2 m}}\right) + \frac{1}{m} \left(\sqrt{\frac{1}{\lambda}} + \sqrt[4]{\frac{1}{\lambda}}\right)\right).$$

Proof. From Lemma B.1 in Srebro *et al.* [2010], we know that for any H -smooth non-negative function $f : \mathbb{R} \rightarrow \mathbb{R}_+$ and any $x, y \in \mathbb{R}$,

$$|f(x) - f(y)| \leq \sqrt{6H(f(x) + f(y))}|x - y|.$$

Suppose f is bounded by $M > 0$, we can easily conclude that f is also L -Lipschitz continuous with $L = \sqrt{12HM}$. Thus, we can apply Theorem 1 to obtain a generalization bound. It turns out above bound can be sometimes tighter than that obtained by directly analyzing the smoothness condition in Theorem 1 [Kuzborskij and Orabona, 2017]. \square

Remark 7. It is noteworthy to mention that we deal with the *non-convex* formulation. Essentially, the loss is not necessarily convex in our analysis. We only assume a bounded and Lipschitz condition (in Theorem 1) or smooth condition (in Corollary 1) for the loss function, along with strongly convexity condition for regularizer. These two conditions can be easily satisfied by common models. For example, in SVMs we use ℓ_2 regularization, which is 2-strongly convex, and the hinge loss $\ell(z, y) = [1 - yz]_+$, which is 1-Lipschitz.

Remark 8. The main techniques in the proof are inspired by Kuzborskij and Orabona [2017], but we differ in three aspects. First, we only assume the Lipschitz condition for loss function, and do not assume and utilize the smoothness as Kuzborskij and Orabona [2017]. Second, our analysis is carried out more scrutinizingly but with simpler proof, and can be easily extended to the smooth loss function case (Corollary 1). Our analysis obtain a slightly better bound by a constant factor, though in the same order with theirs. Moreover, our analysis is extended into multi-class scenarios in Section C.

Appendix C Multi-Class Model Reuse Learning

In this section, we extend the generalization analysis from binary model reuse learning to multi-class case, and provide theoretical analysis and corresponding proofs.

C.1 Rademacher Complexity of Lipschitz Loss Function Family in Multi-Class Case

Lemma 7. Let $H \subseteq \mathbb{R}^{\mathcal{X} \times \mathcal{Y}}$ be a hypothesis set with $\mathcal{Y} = \{1, 2, \dots, c\}$. Assume that the non-negative loss function $\ell : \mathbb{R} \rightarrow \mathbb{R}_+$ is L -regular loss function. Given a set of models $\{h_1, h_2, \dots, h_p\}$ with $\mathbf{h}_p(\mathbf{x}) := [h_1(\mathbf{x}), h_2(\mathbf{x}), \dots, h_p(\mathbf{x})]^\top$, and h_p is a linear combination of previous models, i.e., $h_p(\mathbf{x}) = \langle \boldsymbol{\beta}, \mathbf{f}(\mathbf{x}) \rangle$. Define the feasible set $\mathcal{W} = \{\mathbf{w} : \Omega(\mathbf{w}) \leq \alpha \hat{R}_S(h_p)\}$ and $\mathcal{V} = \{\boldsymbol{\beta} : \Omega(\boldsymbol{\beta}) \leq \rho\}$, let the loss function family associated with hypothesis set \mathcal{H} is defined as

$$\mathcal{L} = \{(\mathbf{x}, y) \rightarrow \ell(\rho_{h_{\mathbf{w}, p}}(\mathbf{x}, y)) : \mathbf{w} \in \mathcal{W} \wedge \boldsymbol{\beta} \in \mathcal{V}\},$$

and let S be a sample of m points drawn i.i.d. according to distribution \mathcal{D} , then we have

$$\mathfrak{R}_m(\mathcal{L}) \leq 2Lc^2 \sqrt{\frac{B^2 \alpha R_p + C^2 \lambda \rho}{\lambda m}}. \quad (27)$$

where $R_p = R(h_p)$, $B = \sup_{\mathbf{x} \in \mathcal{X}} \|\mathbf{x}\|_*$ and $C = \sup_{\mathbf{x} \in \mathcal{X}} \|\mathbf{h}_p(\mathbf{x})\|_*$.

Proof. The loss function family associated with hypothesis set \mathcal{H} is defined as

$$\mathcal{L} = \{(\mathbf{x}, y) \rightarrow \ell(\rho_h(\mathbf{x}, y)) : h \in \mathcal{H} \wedge R(h) \leq r\}.$$

And the empirical Rademacher complexity of \mathcal{L} can be calculated as,

$$\begin{aligned}\hat{\mathfrak{R}}_S(\mathcal{L}) &= \frac{1}{m} \mathbb{E}_\sigma \left[\sup_{h \in \mathcal{H}} \sum_{i=1}^m \sigma_i \ell(\rho_h(\mathbf{x}_i, y_i)) \right] \\ &\leq \frac{L}{m} \mathbb{E}_\sigma \left[\sup_{h \in \mathcal{H}} \sum_{i=1}^m \sigma_i \rho_{h_{W,p}}(\mathbf{x}_i, y_i) \right]\end{aligned}\quad (28)$$

$$\leq \frac{L}{m} \sum_{y \in \mathcal{Y}} \mathbb{E}_\sigma \left[\sup_{h \in \mathcal{H}} \sum_{i=1}^m \sigma_i \rho_{h_{W,p}}(\mathbf{x}_i, y) \right]\quad (29)$$

$$= \frac{L}{m} \sum_{y \in \mathcal{Y}} \left\{ \mathbb{E}_\sigma \left[\sup_{h \in \mathcal{H}} \sum_{i=1}^m \sigma_i \left(h_{W,p}(\mathbf{x}_i, y) - \max_{y' \neq y} h_{W,p}(\mathbf{x}_i, y') \right) \right] \right\}\quad (30)$$

$$\leq \frac{L}{m} \sum_{y \in \mathcal{Y}} \left\{ \mathbb{E}_\sigma \left[\sup_{h \in \mathcal{H}} \sum_{i=1}^m \sigma_i h_{W,p}(\mathbf{x}_i, y) \right] + \mathbb{E}_\sigma \left[\sup_{h \in \mathcal{H}} \sum_{i=1}^m \sigma_i \max_{y' \in \mathcal{Y} \setminus y} h_{W,p}(\mathbf{x}_i, y') \right] \right\}\quad (31)$$

$$\leq \frac{L}{m} \sum_{y \in \mathcal{Y}} \left\{ \mathbb{E}_\sigma \left[\sup_{W \in \mathcal{W}} \sum_{i=1}^m \sigma_i h_{W,p}(\mathbf{x}_i, y) \right] + \sum_{y' \in \mathcal{Y} \setminus y} \mathbb{E}_\sigma \left[\sup_{W \in \mathcal{W}} \sum_{i=1}^m \sigma_i h_{W,p}(\mathbf{x}_i, y') \right] \right\}\quad (32)$$

$$= \frac{Lc^2}{m} \mathbb{E}_\sigma \left[\sup_{W \in \mathcal{W}} \sum_{i=1}^m \sigma_i (\langle \mathbf{w}_y, \mathbf{x}_i \rangle + \langle \boldsymbol{\beta}, \mathbf{h}_p(\mathbf{x}_i) \rangle) \right]\quad (33)$$

$$\leq \underbrace{\frac{Lc^2}{m} \mathbb{E}_\sigma \left[\sup_{W \in \mathcal{W}} \sum_{i=1}^m \langle \mathbf{w}_y, \sigma_i \mathbf{x}_i \rangle \right]}_{\text{term (a)}} + \underbrace{\frac{Lc^2}{m} \mathbb{E}_\sigma \left[\sup_{\boldsymbol{\beta} \in \mathcal{V}} \langle \boldsymbol{\beta}, \sigma_i \mathbf{h}_p(\mathbf{x}_i) \rangle \right]}_{\text{term (b)}}\quad (34)$$

Here, (28) holds due to the fact that loss function ℓ is L -Lipschitz, and thus we can apply Talagrand's Comparison Inequality [Ledoux and Talagrand, 2013; Mohri *et al.*, 2012] to relate the Rademacher complexity of loss family to margin function family. (29), (31) and (34) hold due to the sub-additivity of supremum function. (30) is an application of margin definition. (32) holds due to Lemma 4.

In the following, we proceed to bound two terms in (34), i.e., term (a) and term (b). The basic idea is essentially the same as the technique in (23) and (24), a slight trick here is that we need to introduce an auxiliary vector regularizer, the Euclidean norm $\Omega_{\text{aux}}(\mathbf{w}) = \frac{1}{2} \|\mathbf{w}\|^2$, to establish the connection between Frobenius norm of matrix and Lemma 3, since Lemma 3 is designed for vector norm.

Similarly, we introduce the variable t_1 and t_2 into two Rademacher complexity term, i.e., term (a) and term (b), separately. Note that the Euclidean norm $\Omega_{\text{aux}}(\mathbf{w}) = \|\mathbf{w}\|^2$ is 1-strongly convex function and its dual norm is itself.

$$\begin{aligned}& \frac{Lc^2}{m} \mathbb{E}_\sigma \left[\sup_{W \in \mathcal{W}} \sum_{i=1}^m \langle \mathbf{w}_y, t_1 \sigma_i \mathbf{x}_i \rangle \right] \\ & \leq \frac{Lc^2}{m} \mathbb{E}_\sigma \left[\frac{t_1^2}{2} \sum_{i=1}^m \frac{1}{2} \|\sigma_i \mathbf{x}_i\|^2 + \sup_{\mathbf{w}_y \in \mathcal{W}} \frac{1}{2} \|\mathbf{w}_y\|^2 + \sum_{i=1}^m \frac{1}{2} \langle \nabla \|\mathbf{v}_{1,i-1}\|^2, \sigma_i \mathbf{x}_i \rangle \right]\end{aligned}\quad (35)$$

$$\leq Lc^2 \left(\frac{B^2 t_1^2}{4} + \frac{\alpha \hat{\mathfrak{R}}_S(h_p)}{m} \right)\quad (36)$$

Inequality (35) is obtained by applying Lemma 3 with $f = \Omega_{\text{aux}}$, and $\mathbf{u} = \mathbf{w}_y$ and $\mathbf{v}_i = t_1 \mathbf{x}_i$. And the last step in (36) holds due to the fact that $\sup_{W \in \mathcal{W}} \Omega(W) \leq \alpha \hat{R}_S(h_p)$ and $\sup_{\mathbf{x} \in \mathcal{X}} \|\mathbf{x}\| \leq B$. By dividing t_1 on both sides, and notice that the above upper bound holds for any $t_1 > 0$, we choose a particular t_1 making the upper bound tight,

$$\frac{Lc^2}{m} \mathbb{E}_\sigma \left[\sup_{W \in \mathcal{W}} \sum_{i=1}^m \sigma_i \langle \mathbf{w}, \mathbf{x}_i \rangle \right] \leq \inf_{t_1 > 0} Lc^2 \left(\frac{B^2 t_1}{4} + \frac{\alpha \hat{R}_S(h_p)}{m t_1} \right) = Lc^2 \sqrt{\frac{B^2 \alpha \hat{R}_S(h_p)}{m}}. \quad (37)$$

Similarly, we introduce variable t_2 as tuning parameter for the term (b) with $\mathbf{u} = \mathbf{w}_y$ and $\mathbf{v}_i = t_2 \mathbf{h}_p(\mathbf{x}_i)$,

$$\begin{aligned} & \frac{Lc^2}{m} \mathbb{E}_\sigma \left[\sup_{\beta \in \mathcal{V}} \langle \beta, t_2 \sigma_i \mathbf{h}_p(\mathbf{x}_i) \rangle \right] \\ & \leq \frac{Lc^2}{m} \mathbb{E}_\sigma \left[\frac{t_2^2}{2} \sum_{i=1}^m \frac{1}{2} \|\sigma_i \mathbf{h}_p(\mathbf{x}_i)\|^2 + \sup_{\beta \in \mathcal{V}} \frac{1}{2} \|\beta\|^2 + \sum_{i=1}^m \frac{1}{2} \langle \nabla \|\mathbf{v}_{1:i-1}\|^2, \sigma_i \mathbf{h}_p(\mathbf{x}_i) \rangle \right] \\ & \leq Lc^2 \left(\frac{C^2 t_2^2}{4} + \frac{\rho}{m} \right), \end{aligned}$$

where the last inequality holds due to the fact that $\sup_{\beta \in \mathcal{V}} \|\beta\|^2 \leq 2\rho$ and $\sup_{\mathbf{x} \in \mathcal{X}} \|\mathbf{h}_p(\mathbf{x})\| \leq C$. By dividing t_2 on both sides, and notice that the above upper bound holds for any $t_2 > 0$, we choose a particular t_2 making the upper bound tight,

$$\frac{Lc^2}{m} \mathbb{E}_\sigma \left[\sup_{\beta \in \mathcal{V}} \sum_{i=1}^m \sigma_i \langle \beta, \mathbf{h}_p(\mathbf{x}_i) \rangle \right] \leq \inf_{t_2 > 0} Lc^2 \left(\frac{C^2 t_2}{4} + \frac{\rho}{m t_2} \right) = Lc^2 \sqrt{\frac{C^2 \rho}{m}}. \quad (38)$$

Combing (37) and (38), we obtain obtain the upper bound for $\hat{\mathfrak{R}}_S(\mathcal{L})$. Notice that the square-root function is concave, by applying the Jensen's inequality w.r.t. the both side, we have the following upper bound for Rademacher complexity of loss function family,

$$\begin{aligned} \mathfrak{R}_m(\mathcal{L}) &= \mathbb{E}_S[\hat{\mathfrak{R}}_S(\mathcal{L})] \leq Lc^2 \mathbb{E}_S \left[\sqrt{\frac{B^2 \alpha \hat{R}_S(h_p)}{m}} + \sqrt{\frac{C^2 \rho}{m}} \right] \\ &\leq Lc^2 \left(\sqrt{\frac{B^2 \alpha \mathbb{E}_S[\hat{R}_S(h_p)]}{m}} + \sqrt{\frac{C^2 \rho}{m}} \right) \\ &= Lc^2 \left(\sqrt{\frac{B^2 \alpha R(h_p)}{m}} + \sqrt{\frac{C^2 \rho}{m}} \right) \\ &\leq Lc^2 \sqrt{\frac{2(B^2 \alpha R_p + C^2 \rho)}{m}}. \end{aligned} \quad (39)$$

The last step holds due to the fact that $\sqrt{a} + \sqrt{b} \leq \sqrt{2(a+b)}$, for any $a, b \geq 0$. Hence, we complete the proof. \square

Remark 9. Our analysis follows the framework in Mohri *et al.* [2012], and shows a quadratic dependency on the number of classes c . In fact, it can be improved into linear or radical dependency by utilizing Gaussian complexity [Lei *et al.*, 2015] or vector-contraction inequality for Rademacher complexities [Maurer, 2016], and we will show this in the journal version.

C.2 Proof of Main Theorem

Proof. Since \hat{W} is the optimal solution of regularized ERM in Eq. (10), it is apparently better than the choice $\mathbf{0} \in \mathbb{R}^{d \times c}$,

$$\hat{R}_S(h_{\hat{W},p}) + \lambda\Omega(\hat{W}) \leq \hat{R}_S(h_p) + \lambda\Omega(\mathbf{0}) = \hat{R}_S(h_p),$$

combining the non-negativity of loss function and regularizer, we know that

$$\hat{R}_S(h_{\hat{W},p}) \leq \hat{R}(h_p) \quad \text{and} \quad \Omega(\hat{W}) \leq \hat{R}(h_p)/\lambda.$$

Similar to the proof in (25), we know that the upper bound of risk can be chosen as $r = R_p$, the risk of previous models on target distribution.

Thus, we can apply Lemma 5, obtaining that for $h_{\hat{W},p}$,

$$\begin{aligned} R(h_{\hat{W},p}) - \hat{R}_S(h_{\hat{W},p}) &\leq R_\ell(h_{\hat{W},p}) - \hat{R}_S(h_{\hat{W},p}) \\ &\leq 2\mathfrak{R}_m(\mathcal{L}) + \frac{3M \log(1/\delta)}{4m} + 3\sqrt{\frac{(8\mathfrak{R}_m(\mathcal{L}) + R_p)M \log(1/\delta)}{4m}}. \end{aligned} \quad (40)$$

Setting $\alpha = 1/\lambda$, we have

$$\mathfrak{R}_m(\mathcal{L}) \leq Lc^2 \sqrt{\frac{2(B^2R_p + C^2\lambda\rho)}{\lambda m}}. \quad (41)$$

Plugging (41) into (40), we complete the proof of statements.

$$\begin{aligned} R(h_{\hat{W},p}) - \hat{R}_S(h_{\hat{W},p}) &\leq 2Lc^2 \sqrt{\frac{2(B^2R_p + C^2\lambda\rho)}{\lambda m}} + \frac{3M \log(1/\delta)}{4m} \\ &\quad + 3\sqrt{\frac{\left(8Lc^2 \sqrt{\frac{2(B^2R_p + C^2\lambda\rho)}{\lambda m}} + R_p\right) M \log(1/\delta)}{4m}}. \end{aligned} \quad (42)$$

By some simple derivations and transforms, we complete the proof of main statements. \square

Appendix D More Experimental Results

In this section, we provide more experimental results from the following four aspects:

- (1) weight concentration: we show that the weight distribution learned by `WeightUpdat` largely concentrates on the most relevant previous models.
- (2) recurring concept drift: we conduct performance comparisons on recurring concept drift datasets, and empirically show the effectiveness of `CONDOR` under such circumstance.
- (3) parameter study: we exhibit that our approach is stable to the parameters.
- (4) robustness comparisons: we demonstrate the superiority of proposed approach by performing robustness comparisons over 22 datasets.

Table 3: Detailed information of concept drift in *SEA-recur* dataset. The target concept is determined by $x_1 + x_2 \leq b$, where b changes along with the data stream.

Topic	1 - 100	101 - 200	201 - 300	301 - 400	401 - 500	501 - 600	601 - 700	701 - 800
b	10	10	20	20	20	20	10	10

Table 4: Demonstration of weights concentration phenomenon on synthetic *SEA-recur* dataset. Consider the epoch in 701 - 800, and following shows weights of previous models h_1, h_2, \dots, h_7 .

Iteration	1	2	3	4	5	...	96	97	98	99	100
β_1	0.142	0.159	0.176	0.176	0.192		0.212	0.212	0.212	0.212	0.212
β_2	0.142	0.159	0.176	0.176	0.192		0.472	0.472	0.472	0.472	0.472
β_3	0.142	0.130	0.118	0.118	0.106		4.3E-6	3.5E-6	3.4E-6	2.9E-6	2.3E-6
β_4	0.142	0.130	0.118	0.118	0.106		3.2E-7	2.6E-7	2.1E-7	1.7E-7	1.4E-7
β_5	0.142	0.130	0.118	0.118	0.106		6.4E-6	5.3E-6	5.2E-6	4.3E-6	3.5E-6
β_6	0.142	0.130	0.118	0.118	0.106		4.3E-6	3.5E-6	3.5E-6	2.9E-6	2.4E-6
β_7	0.142	0.159	0.176	0.176	0.192		0.316	0.316	0.316	0.316	0.316

D.1 Weight Concentration

In this paragraph, we present the weight distribution of previous models learned by `WeightUpdate`, in order to show that the weights largely concentrate on the most relevant previous models.

The phenomenon is validated on both synthetic dataset *SEA-recur* and the real-world dataset *Emailing list*. We synthesize the recurring concept drift dataset according to the similar rule of original SEA dataset [Street and Kim, 2001]. That is, there are three attributes x_1, x_2, x_3 , and $0 \leq x_i \leq 10.0$. The target concept is determined by $x_1 + x_2 \leq b$. Table 3 shows the detailed information of concept drift in *SEA-recur* dataset. And Table 4 shows the weight distribution of seven previous models, we can see that the weights concentrate on β_1, β_2 and β_7 , which are the epochs that share the same concept with epoch S_8 .

We also examine the phenomenon on real-world dataset *Emailing list*, whose detailed information of concept drift are shown in Table 5. We can see that the concept drift happens for every 300 round, and in a recurring manner. Let us consider the epoch in 1,200 - 1,500 (epoch 5), actually, the concept in epoch 5 has emerged previously, i.e., it is same as the concepts in epoch 1 and epoch 3. As we can see in Table 6, the weights of four previous model essentially concentrate on the β_1 and β_4 .

Thus, these experiments verify that the returned weight distribution largely concentrates on those previous models who better fit to current data epoch. Essentially, the weight learned by `WeightUpdate` depicts the ‘reusability’ of previous model towards current data.

The weight concentration property plays an important role in making our approach successful. Especially, this is also an evidence to justify why our approach also succeeds in recurring concept drift scenarios, and we will show this in next paragraph.

D.2 Recurring Concept Drift

In this paragraph, we conduct the performance comparison on the *recurring concept drift* scenario, a special sub-type of concept drift, in which previous concepts may disappear and then re-appear in the future. Therefore, previous models may be beneficial for future learning. Previous studies show that one needs to specifically consider the recurring structure, otherwise the performance

Table 5: Detailed information of concept drift in *Emailing list* dataset. There are in total three different topics, “+” indicates the users are interested in it, while “-” indicates not interested in it. Say an example, in the first period (time stamp 0-300), users’ are only interested in messages of the topic medicine.

Topic	1 - 300	301 - 600	601 - 900	901 - 1,200	1,201 - 1,500
Medicine	+	-	+	-	+
Space	-	+	-	+	-
Baseball	-	+	-	+	-

Table 6: Demonstration of weights concentration phenomenon on Email list dataset. Consider the epoch in 1,201 - 1,500, and following reports weights associated with previous models h_1, h_2, h_3, h_4 .

Iteration	1	2	3	4	5	...	296	297	298	299	300
β_1	0.25	0.299	0.345	0.384	0.416		0.5	0.5	0.5	0.5	0.5
β_2	0.25	0.201	0.155	0.116	0.084		1.9E-52	1.3E-52	8.5E-53	5.7E-53	3.8E-53
β_3	0.25	0.299	0.345	0.384	0.416		0.5	0.5	0.5	0.5	0.5
β_4	0.25	0.201	0.155	0.116	0.084		1.9E-52	1.3E-52	8.5E-53	5.7E-53	3.8E-53

will dramatically drop, even for approaches dealing with gradually evolving concept drift.

Datasets. We adopt two popular real-world datasets with recurring concept drift, i.e., *Email list* and *Spam filtering* datasets [Katakis *et al.*, 2008, 2010; Jaber *et al.*, 2013]. Both are datasets extracted from email corpus, and concept is decided by users’ personal interests, which changes in a recurring manner. Detailed information are included in Section E.2.

Comparisons. We compare our proposed approach to approaches in the following four categories, (a) Sliding window based approaches, including SVM-fix (batch implementation by SVM) and NB-sw (update only use the data in sliding window based on incremental Naive Bayes). (b) Ensemble based approaches, including Learn⁺⁺.NSE, DWM and AddExp. (c) Model-Reuse based approaches, including TIX and DTEL. (d) Recurring approaches, which are specifically designed for recurring concept drift scenarios, including Conceptual Clustering and Prediction (CCP) approach, an ensemble method that handle recurring concept drift via similarity clustering [Katakis *et al.*, 2010]. Also, we compare with Dynamic Adaptation to Concept Change (DACC) and its adaptive variant ADACC, detecting recurring concept drift based on a new second-order online learning mechanism [Jaber *et al.*, 2013].

Since codes of CCP, DACC and ACACC are not available, we directly use the results reported in their papers, as we use the whole dataset without any random splitting according to their settings. The experimental results are reported in Table 7, we can see that CONDOR exhibits an encouraging performance on both datasets over three different performance measures. It performs significantly better than general concept drift approaches, and is comparable or even better than those approaches specifically designed for recurring concept drift scenario.

The effectiveness of CONDOR in recurring datasets lies in the effect of *weight concentration*, since our approach guarantees the weight concentrates on the best-fit previous models (See Observation 1).

Table 7: Performance comparison on recurring concept drift datasets, *Email list* and *Spam filtering*.

Category	Approach	<i>Email list</i>			<i>Spam filtering</i>		
		Accuracy	Precision	Recall	Accuracy	Precision	Recall
Window	SVM-fix	71.4	73.7	72.1	88.1	82.0	68.5
	NB-sw	74.7	77.9	73.2	91.9	90.2	77.0
Ensemble	Learn ⁺⁺ .NSE	70.0	76.5	76.5	90.4	84.5	79.6
	DWM	78.2	75.1	81.4	91.9	89.1	84.0
	AddExp	70.4	68.2	71.4	91.3	90.0	80.7
Model-Reuse	TIx	86.2	88.2	88.2	88.5	82.3	69.3
	DTEL	86.2	88.2	88.2	86.3	73.4	71.4
Recurring	CCP	77.5	79.7	77.6	92.3	85.7	83.9
	DACC	76.2	73.8	75.9	94.7	95.1	97.8
	ADACC	77.5	75.2	77.2	94.9	95.6	97.6
Ours	CONDOR	95.6	93.2	99.8	95.4	91.1	90.8

D.3 Parameter Study

In this paragraph, we study the effects of parameters in influencing final accuracy. There are three parameters who play a crucial role in the procedure of CONDOR, and they are model pool size K , regularization coefficient λ and step size η .

Model Pool Size. set the value of model pool size K from 5 to 50, and conduct the experiments on all real-world datasets⁶ for 10 times, and plot the mean and standard variance of predictive accuracy with respect to different parameter K values in Figure 3(a). We can see that the predictive accuracy rises up as the model pool size increases, and is not benefit from even larger model pool. Although a larger K might be benign for performance improvement, the memory cost will also significantly increase with a larger K . In this paper, we set default value of model pool size K as 25.

Regularization Coefficient. We set the value of regularization coefficient λ from 2×10^{-6} to 2×10^6 , and conduct the experiments on all real-world datasets for 10 times, and plot the mean and standard variance of predictive accuracy with respect to different parameter λ values in Figure 3(b). We can see that when we set a relative large λ value, all datasets basically achieve the best performance, and are not sensitive to the λ value. This accords with our intuition, since the λ value represents a trade-off between empirical loss and biased regularization term, a larger value addresses more importance on biased regularization. In other words, when λ is large, it tends to leverage more information to build the new model. Thus, the results in Figure 3(b) implies the effectiveness of model reuse. In this paper, we set default value of regularization coefficient λ as 200.

Step Size. We set the value of step size η from 0 to 1, and conduct the experiments on all real-world datasets for 10 times, and plot the mean and standard variance of predictive accuracy with respect to different parameter η values in Figure 3(c). We can see that when step size is set relatively large, say larger than 0.5, then the performance is satisfying and stable. This phenomenon matches the theoretical suggestion value in Lemma 1, as the theoretical suggestion value can be calculated by $\eta_{\text{theory}} = \sqrt{8 \ln(K/p)} = \sqrt{8 \ln(25)/50} \approx 0.718$, where K is the model size default as 25 and p is epoch size default as 50. In this paper, we set default value of step size

⁶Here, we do not include GasSensor (multi-class) and Covtype (extremely large) datasets. Thus, their default settings epoch size is set as $p = 200$, different from others, as we have mentioned before.

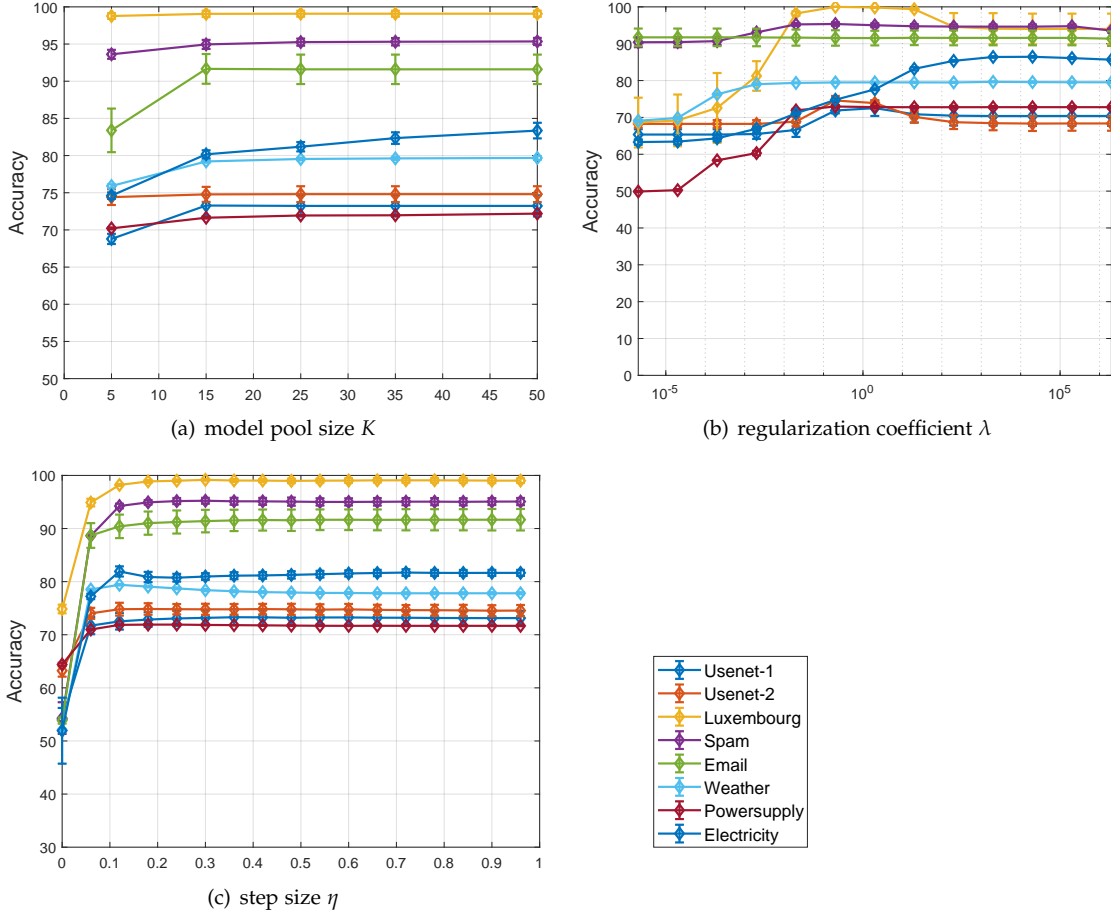


Figure 3: Parameter study on different datasets.

λ as 0.75.

D.4 Robustness Comparisons

Additionally, we conduct robustness comparisons on all approaches over 22 datasets. The robustness measures the performance of a particular approach over all datasets. Concretely speaking, for a particular algorithm $algo$, similar to definition in Vlachos *et al.* [2002], the robustness here is defined as the proportion between its accuracy and the smallest accuracy among all compared algorithms,

$$r_{algo} = \frac{acc_{algo}}{\min_{\alpha} acc_{\alpha}}.$$

Apparently, the worst algorithm has $r_{algo} = 1$, and the others have $r_{algo} \geq 1$, the greater the better. Hence, the sum of r_{algo} over all datasets indicates the robustness of for algorithm $algo$. The greater the value of the sum, the better the performance of the algorithm.

We plot the robustness comparison for five compared approaches and CONDOR over 22 datasets in Figure 4. From the figure, we can see that CONDOR achieves the best over all datasets, both ensemble category and model-reuse category approaches. In particular, our approach shows a

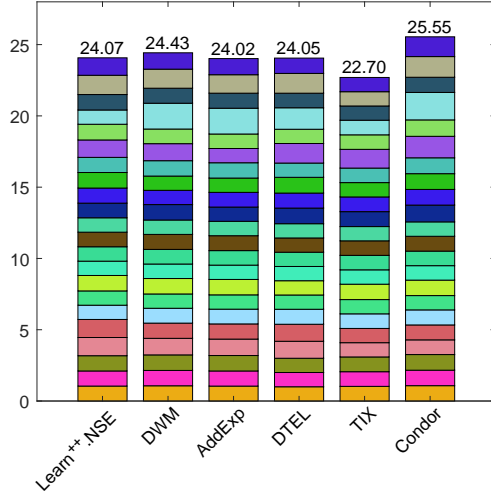


Figure 4: Robustness comparisons of accuracy on five compared approaches and CONDOR over 22 datasets with concept drift.

significant advantage over DTEL and TIX, which verifies the effectiveness of our model reuse strategy.

Appendix E Dataset Descriptions

In this section, we provide detailed descriptions of datasets with concept drift, which are adopted in the experiments.

E.1 Descriptions of Synthetic Datasets

In the experiments, we adopt four commonly used synthetic datasets and their variants: SEA (SEA200A, SEA200G and SEA500G), CIR500G, SIN500G and STA500G.

The first family is SEA dataset Street and Kim [2001], which consists of three attributes x_1, x_2, x_3 , and $0 \leq x_i \leq 10.0$. The target concept is determined by $x_1 + x_2 \leq b$. For the three variants, there are 24,000 instances. The drift period of SEA200A and SEA200G is 200, and for SEA500G, the drift period is 500. ‘A’ indicates $b \in \mathcal{A}$ and ‘G’ indicates $b \in \mathcal{G}$, where $\mathcal{A} = \{10, 7, 3, 7, 10, 13, 16, 13\}$ and $\mathcal{G} = \{10, 8, 6, 8, 10, 12, 14, 12\}$.

The other three synthetic datasets are

CIR500G is a variant of CIRCLE datasets [Elwell and Polikar, 2011], which applies a circle as the decision boundary in a 2-D feature space and simulates concept drift by changing the radius of the circle. The target label is $x_1 + x_2^2 \leq r$ with $r = \{3, 2.5, 2, 2.5, 3, 3.5, 4, 3.5\}$. The drift period is 500.

SIN500G is a variant of SINE datasets [Elwell and Polikar, 2011], which applies a sine curve as the decision boundary in a 2-D feature space and simulates concept drift by changing the angle. The target label is $\sin(x_1 + \theta) \leq x_2$ with $\theta_0 = 0$ and $\Delta\theta = \pi/60$. The drift period is 500.

STA500G is a variant of STAGGER Boolean Concepts [Schlimmer and Granger, 1986], which generate the data with categorical features using a set of rules to determine the class label. Details is included in Sun *et al.* [2018]. The drift period is 500.

The other six synthetic datasets are 1CDT, 1CHT, UG-2C-2D, UG-2C-3D, UG-2C-5D and GEARS-2C-2D. Their basic information are reported in Table 1. For more details, one can refer to the paper [de Souza *et al.*, 2015].

E.2 Descriptions of Real-World Datasets

In the experiments, we adopt nine real-world datasets: Usenet-1, Usenet-2, Luxembourg, Spam, Email, Weather, Powersupply, Electricity and Coverttype. The number of data items varies from 1,500 to 581,012. Basic statistics are included in Table 1, and we provide detailed descriptions as follows.

- *Usenet* [Katakis *et al.*, 2008] is split into *Usenet-1* and *Usenet-2* which both consist of 1,500 instances with 100 attributes based on 20 newsgroups collection. They simulate a stream of messages from different newsgroups that are sequentially presented to a user, who then labels them according to his/her personal interests.

- *Luxembourg* [Zliobaite, 2011] is constructed by using European Social Survey data. There are 1,900 instances with 32 attributes in total, and each instance is an individual and attributes are formed from answers to the survey questionnaire. The label indicates high or low internet usage.

- *Spam Filtering* [Katakis *et al.*, 2009] is a real-world textual dataset that uses email messages from the Spam Assassin Collection, and boolean bag-of-words approach is adopted to represent emails. It consists of 9,324 instances with 500 attributes, and label indicates spam or legitimate.

- *Email List* [Katakis *et al.*, 2009] is a stream of 1,500 examples and 913 attributes which are words that appeared at least 10 times in the corpus (boolean bag-of-words representation), which are collected from 20 Newsgroup collection. The users' personal interests are changing in a recurring manner.

- *Weather* [Elwell and Polikar, 2011] dataset is originally collected from the Offutt Air Force Base in Bellevue, Nebraska. 18,159 instances are presented with an extensive range of 50 years (1949 – 1999) and diverse weather patterns. Eight features are selected based on their availability, eliminating those with a missing feature rate above 15%. The remaining missing values are imputed by the mean of features in the preceding and following instances. Class labels are based on the binary indicator(s) provided for each daily reading of rain with 18,159 daily readings: 5698 (31%) positive (rain) and 12,461 (69%) negative (no rain).

- *GasSensor* [Vergara *et al.*, 2012] is a dataset contains 4,450 measurements from 16 chemical sensors utilized in simulations for drift compensation in a discrimination task of six gases (six classes) at various levels of concentrations.

- *Powersupply* [Chen *et al.*, 2015] contains three year power supply records including 29,928 instances with 2 attributes from 1995 to 1998, and our learning task is to predict which hour the current power supply belongs to. We relabel into binary classification according to p.m. or a.m.

- *Electricity* [Harries and Wales, 1999] is widely adopted and collected from the Australian New South Wales Electricity Market where prices are affected by demand and supply of the market. The dataset contains 45,312 instances with 8 features. The class label identifies the change of the price relative to a moving average of the last 24 hours.

- *Covertypes* [Gama *et al.*, 2003; Sun *et al.*, 2018] is a real-world data set for describing the observation of a forest area with 51 cartographic variables obtained from US Forest Service (USFS) Region 2 Resource Information System (RIS). Binary class labels are involved to represent the corresponding forest cover type.

- *PokerHand* [Cattral *et al.*, 2002] describes the suits and ranks of a hand of five playing cards, which consists of 1,000,000 instances and 11 attributes. Each card is described using two attributes (suit and rank). Each card is described using two attributes (suit and rank), for a total of 10 predictive attributes. There is one class attribute that describes the "Poker Hand".